



# Numerical study of hydromagnetic convective heat and mass transfer flow of Ethylene Glycol based CuO and Gold Nanofluids in a vertical channel with Hall effects, activation energy and heat generating sources

<sup>1</sup>B. Sreenivasa Reddy, <sup>2</sup>Shahanaz Begum, <sup>3</sup>G.V.Lokeswara Reddy

<sup>1</sup>Associate Professor, Department of Applied Mathematics, Yogivemana University, Kadapa-516005, A.P., India

<sup>2</sup>Research Scholar, Department of Applied Mathematics, Yogivemana University, Kadapa-516005, A.P., India

<sup>3</sup>Lecturer, Department of Physics, Government Degree College, Yerraguntla, A.P., India,

**Abstract :** The present investigate deals with hydromagnetic convective heat and mass transfer flow of rotating Ethylene glycol based CuO, Gold nanofluids with activation energy, variable viscosity, thermal radiation and heat sources. The governing equations have been solved by employed Galarkin finite element analysis with quadratic intropolation function. The velocity, temperature and concentration are shown graphically for different parametric variations. It is found that higher the activation energy parameter( $E_1$ ) smaller the temperature and larger the nanoconcentration in the flow region. The values of  $u, w, \theta$  and  $C$  in Eg-Cuo nanofluid are greater than those in Eg-Gold nanofluid with higher values of nanoparticle volume fraction ( $\phi$ ). Velocities decays in both types of nanofluids with larger values of nanoparticle volume fraction( $\phi$ ).

**Keywords :** Vertical channel, Activation Energy, Heat Sources, Heat and Mass transfer, CuO and Gold Nanofluid.

## 2. INTRODUCTION

Nanofluids are a classification of heat transfer fluids which are engineered suspension nanoparticles (1–100 nm) being dispersed in the fluid. Usually base fluids incorporate water, organic fluids (e.g. ethylene, triethylene and so on) engine oil, polymeric solutions, bio-fluids and other basic fluids. Medium normally utilized as nanoparticles encompass carbon in different structures (e.g. carbon nanotubes, graphite, diamond) metals (e.g. copper, silver, gold), metal oxides (e.g. titania, zirconia) and functionalized nanoparticles. Utilization of nanofluids has found an extensive variety of potential applications. Choi was the first one to study enhancement of thermal conductivity in nanofluids (Choi [8]). The fusion of specialized fluids that are designed towards enhancing the performance of heat exchangers has turned out to be progressively appealing lately. Several authors (Chen et al. [5], Zhou et al. [55], Kabeel et al. [22], Peyghambarzadeh et al. [39], Wongwises [14]) presented an approach to predict the thermal conductivity of fluid containing nano-sized particles and the experimental data and computed thermophysical properties of nanofluids on heat transfer phenomena, based on their rheological properties.

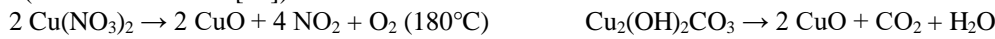
The homotopy analysis method (HAM) to analyze the entropy of a nanofluid consisting of water as the primary fluid and one of four distinct kinds of nanoparticles:  $TiO_2$ ,  $Al_2O_3$ ,  $Cu$ , and  $CuO$  flowing through a stretchable permeable surface. Furthermore, Abolbashari *et al.*, [1] and, Das and Jana [10] and Das *et al.*, [11], Sandeep and Reddy [9], Reddy *et al.*, [42] and Mahanthesh *et al.*, [29], Cheng [6 & 7] investigated the natural convective flow of nanofluids with radiation for moving vertical plate and vertical channel, respectively. Rashidi *et al.*, [14] looks for a lie group solution to the problem of how the nanofluid moves past a horizontal plate reacting chemically.

The vertical channel is an often encountered configuration in thermal engineering equipment, as an example, collectors of solar power, cooling devices of digital and micro-digital equipments and many others. Das *et al.* [10] have considered transient natural convection in a vertical channel filled with nanofluids in the presence of thermal radiation. Fakour *et al.* [15] have described the mixed convection flow of a nanofluid in a vertical channel. Grosan and Pop [19] have presented the fully developed mixed convection in a vertical channel filled with nanofluid. Furthermore, several authors (Maghrebi *et al.* [27], Maïga *et al.* [30, 31], Nield and Kuznetsov [37], Sacheti *et al.* [44], Sheikholeslami and Ganji [48], Sreedevi *et al.* [50], Arundhati *et al.* [2, 4], Sudarsana Reddy *et al.* [52], Mahajan and Arora [28], Nadeem and Saleem [34], Sreedevi and Prasada Rao [49]) have studied the forced convective heat transfer of nanofluids in a porous channel with uniformly heated tube through MHD and permeable channel over a rotating disk through porous medium saturated by Cu-water and Ag-water nanofluid with chemical reaction.

**Copper(II) oxide** or **cupric oxide** is an inorganic compound with the formula  $CuO$ . A black solid, it is one of the two stable oxides of copper, the other being  $Cu_2O$  or copper(I) oxide (cuprous oxide). Copper(II) oxide belongs to the monoclinic crystal system. The copper atom is coordinated by 4 oxygen atoms in an approximately square planar configuration (Forsyth and Hull [16]). The work function of bulk  $CuO$  is 5.3 eV. (Koffyberg and Benko[24]).

It can be formed by heating copper in air at around 300–800 °C:  $2 Cu + O_2 \rightarrow 2 CuO$

For laboratory uses, copper(II) oxide is conveniently prepared by pyrolysis of copper(II) nitrate or basic copper(II) carbonate:(Glemser and Sauer[18])



As a significant product of copper mining, copper(II) oxide is the starting point for the production of many other copper salts. For example, many wood preservatives are produced from copper oxide (Richardson and Wayne[43]). Cupric oxide is used as a pigment in ceramics to produce blue, red, and green, and sometimes gray, pink, or black glazes[Richardson and Wayne[43]]. Due to low bioactivity, negligible copper is absorbed (Baker and David[3]).

The model with potential reactants to produce a chemical reaction minimizing the energy in the chemical system is focused nowadays in the industrial manufacturing of, extrusion of plastic, aerodynamics with rubber sheets crystal growing, geothermal or oil reservoir engineering and so on (Dhlamini et al. [13]). The Arrhenius activation terminology was first indicated by Svante Arrhenius around 1889. One significant measure in free convection boundary layer flows taking into account heat mass transfer together is the specific chemical reactions with finite Arrhenius activation energy (Maleque [32], Netai and Dulal [36]). The effect of activation energy on convective heat transfer flow of nanofluid in vertical channel have analysed by Devasena [12], Gayathri [17], Kathyani and Subramanyam [23], Nagasasikala [35], Satya Narayana and Ramakrishna [46], Madduleti Nagasasikala, Bommanna Lavanya [26 have been analyzed the effects of dissipation and radiation on heat transfer flow of a convective rotating Cuo-water nano-fluid in a vertical channel.

Gold nanoparticles have a variety of applications in medical sciences, including photothermal (PT), gene transfection agents, radiosensitizing, drug delivery, therapeutic etc. Especially in a lab, gold metallic nanoparticles are commonly utilized as a tracer to indicate the existence of certain proteins or DNA in a sample and identify the different antibiotics. They are biocompatible and can deliver heat energy to tumor cells via various therapeutic techniques. Because cancer cells are microscopic, appropriately, nanosized gold nanoparticles were infused into the bloodstream for infiltration and found very effective. Keeping in mind the applications of gold nanoparticles, Nanoparticulate Au catalysts are active under mild conditions, even at ambient temperature or less, and this makes them unique. Use of mixed precious metal catalysts can produce even higher activities than the use of Au alone [Huang et al.[21] & Thompson [53]]. Several authors (Hatami et al [20], Mohamed Ouni et al [33], Shafiq Ahmad et al [47], Srinivas et al [51], Umair Khan et al[54], Bentoto et al. [4]) have discussed the Flow and heat transfer of gold-blood nanofluid in a porous channel with moving/stationary walls and the Computer, Simulation of MHD Blood Conveying Gold Nanoparticles as a Third Grade Non-Newtonian Nanofluid in a Hollow Porous Vessel on Sisko Fluid Flow Containing Gold Nanoparticles through a Porous Curved Surface in the Presence of Radiation and Partial Slip.

In this paper to investigate the combined influence of hydromagnetic convective heat and mass transfer flow of Ethylene Glycol based Cuo and Gold Nanofluid in a vertical channel with Hall effects, activation energy and heat generating sources. The nonlinear coupled equations governing the flow, heat and mass transfer of nanofluid have been solved by Finite element technique with quadratic interpolation functions. The conclusions of the velocity, temperature and concentration have been discussed for different parametric variations.

**2.2. FORMULATION OF THE PROBLEM:**

We consider the steady, three dimensional flow of a nanofluid consisting of a base fluid and small nanoparticles of CuO, Gold in a vertical porous channel with thermal radiation. A uniform magnetic field of strength Ho is applied normal to the plate. It is assumed that there is no applied voltage which implies the absence of an electric field. The flow is assumed to be in the x-direction which is taken along the plane in an upward direction and z-axis is normal to the plate. Also it is assumed that the whole system is rotating with a constant angular velocity vector  $\bar{\Omega}$  about the z-axis. The fluid is assumed to be gray, absorbing emitting but not scattering medium. The radiation heat flux in the x-direction is considered negligible in comparison with that in the z-direction. Due to the fully developed assumption, the flow variables are functions of z and t only. Figure. 1 shows that the problem under consideration and the co-ordinate system.

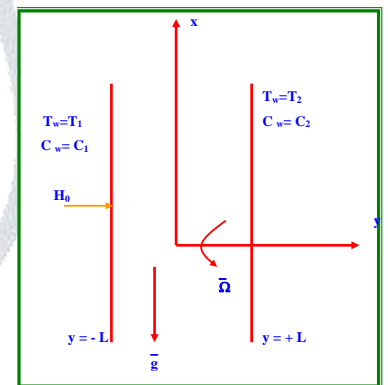


Figure 1 . Schematic diagram of the problem of

In the present problem, the following assumptions have been made: The conservation equation current density  $\nabla \cdot \bar{J} = 0$  gives  $J_z = \text{constant}$ .

Under the above mentioned assumptions, the equation of momentum and thermal energy respectively under Rosseland approximation can be written in dimensional form as :

$$\frac{\partial u}{\partial x} + \frac{\partial v}{\partial y} = 0 \tag{1}$$

$$\rho_{nf} (v \frac{\partial u}{\partial y} - 2\Omega w) = \mu_{nf} (\frac{\partial^2 u}{\partial y^2}) + (\rho\beta_T)_{nf} g(T - T_1) - \frac{\sigma_{nf} B_o^2}{(1+m^2)} (u + mw) \tag{2}$$

$$\rho_{nf} (v \frac{\partial w}{\partial y} + 2\Omega u) = \mu_{nf} (\frac{\partial^2 w}{\partial y^2}) + \frac{\sigma_{nf} B_o^2}{(1+m^2)} (mu - w) \tag{3}$$

$$(\rho C_p)_{nf} (v \frac{\partial T}{\partial y}) = \frac{k_{nf}}{\rho_f C_p} \frac{\partial^2 T}{\partial y^2} - \frac{1}{\rho_f C_p} \frac{\partial(q_R)}{\partial y} + Q_H(T - T_1) + 2\mu_{nf} [(\frac{\partial u}{\partial y})^2 + (\frac{\partial w}{\partial y})^2] + \frac{\sigma_{nf} \mu_e H_o^2}{1+m^2} (u^2 + w^2) \tag{4}$$

$$u \frac{\partial C}{\partial y} = D_B \frac{\partial^2 C}{\partial y^2} + \frac{D_T}{T_\infty} (\frac{\partial^2 T}{\partial y^2}) - kc(C - C_\infty) (\frac{T}{T_o})^n \text{Exp}(-\frac{E_a}{KT}) \tag{5}$$

The boundary conditions are:

$$u(\pm L) = 0, w(\pm L) = 0, T(-L) = T_1, T(+L) = T_2, C'(-L) = C_1, C'(+L) = C_2 \tag{6}$$

where  $(u, v, w)$  are the velocity components along the  $(x, y, z)$  directions respectively.  $T, C$  are the temperature and Concentration in the fluid region.  $Q_H$  is the strength of the heat source,  $\sigma_{nf}$  is the effective electrical conductivity,  $\mu_{nf}$  is the effective magnetic permeability,  $\rho_{nf}$  is the effective fluid density,  $H_0$  is the strength of the magnetic field,  $\beta_T$  is the effective thermal volumetric coefficient of expansion,  $k_c$  is the chemical reaction coefficient,  $D_B$  is the solution diffusivity of the medium,  $D_T$  is the thermal diffusion ratio,  $K$  is the Stefan-Boltzmann constan, the concentration susceptibility,  $C_p$  is the specific heat at constant pressure,  $T_0$  is the mean fluid temperature and  $q_R$  is the radiative heat flux.  $m = \frac{\sigma B_0}{en_c}$  is the Hall parameter.  $E_a$  is the activation energy coefficient.

The properties of the nanofluids are defined as follows:

$$\begin{aligned} \mu_{nf} &= \mu_f / (1 - \phi)^{2.5} & \alpha_{nf} &= \frac{k_{nf}}{(\rho C_p)_{nf}} & \rho_{nf} &= (1 - \phi)\rho_f + \phi\rho_s \\ (\rho C_p)_{nf} &= (1 - \phi)(\rho C_p)_f + \phi(\rho C_p)_s & (\rho\beta)_{nf} &= (1 - \phi)(\rho\beta)_f + \phi(\rho\beta)_s \\ k_{nf} &= \frac{k_f(k_s + 2k_f - 2\phi(k_f - k_s))}{(k_s + 2k_f + 2\phi(k_f - k_s))}, & \sigma_{nf} &= \left(\sigma_f + \frac{3(\sigma_f - \sigma_s)\phi}{(\sigma_s + 2\sigma_f)}\right), \end{aligned} \tag{7}$$

where the subscripts  $nf, f$  and  $s$  represent the thermo physical properties of the nanofluid, base fluid and the nanosolid particles respectively and  $\phi$  is the solid volume fraction of the nanoparticles. The thermo physical properties of the nanofluid are given in Table 1.

The thermo physical properties of the nanofluids are given in Table 1 (See *Oztop and Abu-Nada* [2008]).

**Table – 1 : Physical Properties of nanofluids**

Physical properties	Fluid phase (Water)	Cu0-nanofluid	Gold-nanofluid
$C_p$ (j/kg K)	4179	<b>6320</b>	<b>19300</b>
$\rho$ (kg m <sup>3</sup> )	997.1	<b>531.9</b>	<b>129.1</b>
$k$ (W/m K)	0.613	<b>76.5</b>	<b>318</b>
$\beta \times 10^{-5}$ 1/k)	21	1.80	<b>1.40</b>
$\sigma$	<b>0.05</b>	<b>2.7</b>	<b>4.52</b>

We consider the solution of equation(1) as:

$$v = -v_0 \tag{8}$$

We introduce the following dimensionless variables:

$$z' = \frac{z}{L}, u' = \frac{u}{v_0}, w' = \frac{v}{v_0}, \theta = \frac{T - T_1}{T_2 - T_1}, C = \frac{C' - C_1}{C_2 - C_1} \tag{9}$$

Equations(2)-(4) in the non-dimensional form are

$$0 = \left( \frac{\partial^2 u}{\partial y^2} \right) + \left[ A_1 A_3 \left( -S \frac{\partial u}{\partial z} + 2Rw \right) + A_1 A_4 G\theta - A_1 A_6 \frac{M^2}{1+m^2} (u + mw) \right] \tag{10}$$

$$0 = \left( \frac{\partial^2 w}{\partial y^2} \right) + \left[ A_1 A_3 \left( S \frac{\partial w}{\partial y} - 2Ru \right) - A_1 A_6 \frac{M^2}{1+m^2} (mu - w) \right] \tag{11}$$

$$0 = \left( 1 + \frac{4Rd}{3} \right) \frac{\partial^2 \theta}{\partial y^2} + S Pr \frac{\partial \theta}{\partial y} - Q\theta + Ec Pr \left[ \left( \frac{\partial u}{\partial y} \right)^2 + \left( \frac{\partial w}{\partial y} \right)^2 \right] + \tag{12}$$

$$+ Ec Pr \frac{M^2}{1+m^2} (u^2 + w^2)$$

$$0 = \frac{\partial^2 C}{\partial y^2} + S Sc \frac{\partial C}{\partial y} - \gamma C (1 + n\delta\theta) Exp\left(-\frac{E_1}{1+\delta\theta}\right) + Sc So \frac{\partial^2 \theta}{\partial y^2} \tag{13}$$

Where

$$G = \frac{\beta g (T_2 - T_1) L^2}{\mu_f \nu_0},$$

$$S = \frac{\nu_0 L}{\mu_f}, M = \frac{\sigma \mu_e^2 H_0^2 L^2}{\rho_f \mu_f}, Q = \frac{Q_H L^2}{k_f}, Rd = \frac{4\sigma^* T_\infty^3}{\beta_R k_f}, So = \frac{D_B K_T (C_2 - C_1)}{T_m (T_2 - T_1)}, \gamma = \frac{k_c L^2}{D_B}$$

$$G = \frac{\beta_T g (T_2 - T_1) L^3}{\nu^2} \text{ (Grashof number)}, M^2 = \frac{\sigma \mu_e^2 H_0^2}{L} \text{ (Magnetic parameter)}, Rd = \frac{4\sigma^* T_\infty^3}{\beta_R k_f} \text{ (Radiation parameter)},$$

$$R = \frac{\Omega L}{\nu} \text{ (Rotation parameter)}, Q = \frac{Q_H \nu}{bk_f} \text{ (Heat source parameter)}, S = \frac{\nu_0 L}{\mu_f} \text{ (Suction parameter)}, Pr = \frac{\mu_f C_p}{k_f} \text{ (Prandtl number)}, Le = \frac{\nu}{D_B} \text{ (Lewis number)}, \gamma = \frac{k_c \nu}{L} \text{ (Chemical reaction parameter)}, Sr = \frac{D_T (T_2 - T_1)}{T_0 C_p (C_2 - C_1)} \text{ (Soret parameter)},$$

$$\theta_w = \frac{T}{T_0}, \delta = \theta_w - 1, (\text{Temperature difference ratio}), E_1 = \frac{E_a}{KT_0} \quad (\text{Activation energy parameter}),$$

$$A_1 = (1-\phi)^{2.5} \quad A_2 = \frac{k_{nf}}{k_f}, \quad A_3 = 1 - \phi + \phi \left( \frac{\rho_s}{\rho_f} \right), \quad A_4 = 1 - \phi + \phi \left( \frac{(\rho\beta)_s}{(\rho\beta)_f} \right), \quad A_5 = 1 - \phi + \phi \left( \frac{(\rho C_p)_s}{(\rho C_p)_f} \right), \quad A_6 = \left( 1 + \frac{3(1-\sigma)\phi}{(\sigma+2)} \right), \quad \sigma = \frac{\sigma_s}{\sigma_f}$$

The boundary conditions reduce to

$$u(\pm 1) = 0, v(\pm 1) = 0, \theta(-1) = 0, \theta(+1) = 1, C(-1) = 0, C(+1) = 1 \tag{14}$$

**3. FINITE ELEMENT ANALYSIS**

The finite element analysis with quadratic polynomial approximation functions is carried out along the axial distance across the vertical channel. The behavior of the velocity, temperature and concentration profiles has been discussed computationally for different variations in governing parameters. The Galerkin method has been adopted in the variational formulation in each element to obtain the global coupled matrices for the velocity, temperature and concentration in course of the finite element analysis.

Choose an arbitrary element  $e_k$  and let  $u^k, v^k, \theta^k$  and  $C^k$  be the values of  $u, v, \theta$  and  $C$  in the element  $e_k$ . We define the error residuals as

$$E_u^k = \frac{d}{dy} \left( \frac{du^k}{dy} \right) + [A_1 A_4 G(\theta^k) - S u^k - 2R w^k + Ec Pr \left[ \left( \frac{\partial u^k}{\partial y} \right)^2 + \left( \frac{\partial w^k}{\partial y} \right)^2 \right] + A_1 A_6 \frac{M^2}{1+m^2} (u^k)^2 + (w^k)^2] \tag{15}$$

$$E_v^k = \frac{d}{dy} \left( \frac{dw^k}{dy} \right) + \left[ -S \frac{dw^k}{dy} - 2R u^k + A_1 A_6 \frac{M^2}{1+m^2} w^k \right] \tag{16}$$

$$E_\theta^k = \frac{A_2}{Pr} \frac{d}{dy} \left( \frac{d\theta^k}{dy} \right) - S Pr \theta^k A_3 u^k - Q \theta^k + Ec \left[ \left( \frac{du^k}{dy} \right)^2 + \left( \frac{dw^k}{dy} \right)^2 \right] + Ec \frac{M^2}{1+m^2} ((u^k)^2 + (w^k)^2) \tag{17}$$

$$E_c^k = \frac{d}{dz} \left( \frac{dC^k}{dz} \right) - S S_c \frac{dC^k}{dz} - \gamma C^k (1 + n \delta \theta^k) \exp \left( -\frac{E_1}{1 + \delta \theta^k} \right) + S_c S_o \frac{d}{dz} \left( \frac{d\theta^k}{dz} \right) \tag{18}$$

where  $u^k, w^k, \theta^k$  &  $C^k$  are values of  $u, w, \theta$  &  $C$  in the arbitrary element  $e_k$ . These are expressed as linear combinations in terms of respective local nodal values.

$$u^k = u_1^k \psi_1^k + u_2^k \psi_2^k + u_3^k \psi_3^k, \quad w^k = w_1^k \psi_1^k + w_2^k \psi_2^k + w_3^k \psi_3^k, \quad \theta^k = \theta_1^k \psi_1^k + \theta_2^k \psi_2^k + \theta_3^k \psi_3^k, \quad C^k = C_1^k \psi_1^k + C_2^k \psi_2^k + C_3^k \psi_3^k \tag{19}$$

where  $\psi_1^k, \psi_2^k, \dots$  etc are Lagrange’s quadratic polynomials.

Galerkin’s method is used to convert the partial differential Equations (15) – (18) into matrix form of equations which results into 3x3 local stiffness matrices. All these local matrices are assembled in a global matrix by substituting the global nodal values and using inter element continuity and equilibrium conditions. The resulting global matrices have been solved by iterative procedure until the convergence i.e  $|u_{i+1} - u_i| < 10^{-6}$  is obtained.

**4. COMPARISON:**

Table 2 : In absence of  $m=0, Q=0, Ec=0, E1=0$  the nusselt number in Copper(Cuo) and Gold (Au)– Eg agree with the results of Madduleti Nagasasikala, Bommanna Lavanya [26] & Srinivas et al [51]

$\phi$	Rd	$\theta'$ (+1) Madduleti Nagasasikala, Bommanna Lavanya [26] Cuo-Eg Nanofluid	$\theta'$ (+1) Srinivas et al [51] Au(Gold)-Eg Nanofluid	Present Results ( $\theta'$ (+1)) Cuo-Eg Nanofluid	$\theta'$ (+1) Present results Au(Gold)-Eg Nanofluid
0.05	0.5	0.49456	0.49499	<b>0.49462</b>	<b>0.49489</b>
0.10	0.5	0.49476	0.49502	<b>0.49481</b>	<b>0.49495</b>
0.12	0.5	0.49640	0.49506	<b>0.49653</b>	<b>0.49504</b>
0.05	1.0	0.48842	<b>0.48124</b>	<b>0.48846</b>	<b>0.48890</b>
0.05	1.5	0.49577	<b>0.46097</b>	<b>0.49584</b>	<b>0.49644</b>

**5.RESULTS AND DISCUSSION:**

In this analysis an attempt has been to investigate the effect of activation energy, thermo diffusion, dissipation, Hall current effects on the convective heat and mass transfer flow of rotating Ethylene Glycol based Cuo and Gold nanofluids in the presence of heat generating sources. The non-linear, coupled equations governing the flow have been executed by employing Runge-Kutta –fourth order along with Shooting technique. The behaviour of axial velocity( $u$ ), cross flow velocity( $w$ ), temperature( $\theta$ ) and nanoconcentration( $\Phi$ ) have been discussed through different profiles. The rate of heat and mass transfer on the walls have been evaluated for different parametric variations (Grashof number(G),Magnetic parameter(M), Hall currents( $m$ ), porous permeability parameter(K), suction parameter(S), Rotation parameter(R),radiative heat flux(Rd), Eckert number(Ec), heat source(Q), nanoparticle volume fraction( $\phi$ ),Prandtl number(Pr), molecular diffusivity( $Sc$ ), thermo-diffusion (Sr), chemical reaction ( $\gamma$ ), radiation absorption parameter(Q1), activation energy(E1), temperature difference ratio( $\delta$ ), index number(n), skin friction components ( $\tau_x, \tau_z$ ),Nusselt(Nu) and Sherwood(Sh) numbers).

$u, w$  experience upsurge with rise in  $G$  in both types Eg based CuO and Gold nanofluids (fig.2a&2b).  $\theta$  &  $\Phi$  reduces with increase in  $G$  in both types of nanofluids (figs.2c&2d). This is due to the fact the rise in  $G$  leads to increase in the thickness of the thermal and decay of the solutal boundary layers. In all the variations the values of flow variables ( $u, w, \theta$  and  $\Phi$ ) in Eg-Cuo nanofluid are relatively greater than those in Eg-Gold nanofluids at all points in the flow region.

Figs.3a-3d, Higher  $M$ , smaller  $u$  and larger  $w$  in Eg based CuO nanofluid while in Eg Gold nanofluid it reduces in the flow region (figs.3a&3b). The thermal boundary layer becomes thicker and the solutal layer becomes thinner with rising values of  $M$  (figs.3c&3d). The values of  $u, \Phi$  in Eg-Cuo nanofluid are relatively greater than those in Eg-Gold nanofluid while the values of  $\theta$  in Eg-Cuo nanofluid are smaller than those in Eg-Gold nanofluid in the flow region.

Fig.4a-4d  $\Phi$ . Increase in  $m$  reduces  $u$  and  $\Phi$  in the flow region  $(-1,0,0.5)$  and enhances in the region  $(0.5,1,0)$  in Eg-Cuo and Eg-Gold nanofluids (figs.4a&4d). A reversed behaviour is observed in  $w$  and  $\theta$  with increasing values of  $m$  in both the nanofluids (figs.4b & 4c). The values of  $f', g, \theta$  and  $C$  in Eg based CuO nanofluid are relatively greater than those in Eg-Gold nanofluid

$w$ , and  $\theta$  depreciates in the in flow region  $(-1,0,0.5)$  and enhances in the region  $(0.5,1,0)$  with higher values of  $K$  (figs.5b, 5c). The thickness of the thermal boundary layer grows in Eg- CuO nanofluid and decays in Eg- Gold nanofluid (fig.5c).  $u, w, \Phi$  in Eg-Cuo nanofluid are relatively greater than those in Eg-Gold nanofluid while in the case of temperature, an opposite effect is noticed in its behaviour.

$S$  leads to a depreciation in  $u, \theta$  and  $\Phi$  in the entire flow region in both types of nanofluids. (figs.6a,6c,6d).  $w$  reduces in the flow region  $(-1,0,0.5)$  and enhances in the region  $(0,5,1,0)$  with increase in  $S$  in both types of nanofluids. (fig.6b).  $u, w, \Phi$  in Eg-Cuo nanofluid are relatively greater than those in Eg-Gold nanofluid.  $\theta$  in Eg-Cuo nanofluid are lesser than those in Eg-Gold nanofluid.

Higher the Coriolice force ( $R$ ) smaller  $u$  and  $\Phi$  in Eg based CuO and Eg-Gold nanofluid (figs.7a&7d).  $w$  and  $\theta$  experience an enhancement with larger values of  $R$  in both types of nanofluids. Thus the thermal boundary layer becomes thicker and solutal layer becomes thinner with higher values of  $R$  in Eg based CuO and Eg-Gold nanofluids. The values of  $u, \Phi$  in Eg- CuO nanofluid are relatively are smaller than those in Eg- Gold nanofluid while in the case of  $w, \theta$ , an opposite effect is noticed in its behaviour.

An augmentation in  $u, w, \theta$  and reduction in  $\Phi$  with larger values of  $Rd$  (figs.8a-d) in both types of nanofluids. The values of  $u, w$ , in Eg based Gold nanofluid are relatively smaller than those in Eg based CuO nanofluid while in the case of  $\theta$  its values in Eg-Gold nanofluid are greater than those in Eg-Cuo nanofluid.

Higher the dissipative energy, larger  $u, w, \theta$  (figs.9a-9c) while  $\Phi$  depreciate in the entire flow region in both types of nanofluids (fig.9d). The values of  $u, w, \theta$  in Eg-Cuo nanofluid are relatively smaller than those in Eg-Gold nanofluid while the opposite effect is noticed in  $\Phi$  in Eg based CuO and Gold nanofluids.

Figs.10a-10d, In  $Q > 0$ ,  $u$  reduces in the flow region  $(-1,0,0.5)$  and enhances in the region  $(0.5,1,0)$  in both types of nanofluids.  $w, \theta, \Phi$  upsurge in the flow region  $(-1,0,0.5)$  and reduces in the region  $(0.5,1,0)$  in Eg-Cuo and Gold nanofluids (10b-10d). The values of  $u, w, \theta$  in Eg-Cuo nanofluid are smaller than those in Eg based Gold nanofluid while in Eg based CuO nanofluid, the values of  $\Phi$  in Eg- Gold nanofluid are relatively smaller than those in Eg- CuO nanofluid.

Rising values of  $\phi$  leads to depreciation in  $u, w$  and  $\Phi$  in the entire flow region while  $\theta$  upsurgues in the flow region in Eg-Cuo nanofluid and reduces in Eg-Gold nanofluid (figs.11a-11d). The values of  $u, w, \theta$  and  $\Phi$  in Eg based CuO nanofluid are relatively greater than those in Eg-Gold nanofluid.

Figs.12a-12d in  $Pr$ ,  $u, w, \theta$  reduce,  $\Phi$  upsurgues in Eg based CuO and Gold nanofluids The values of  $u, w, \theta$  in Eg based CuO nanofluid are relatively greater than those in Eg based Gold nanofluid while in the case of  $\Phi$ , an reversed effect is noticed.

From fig.13c-13d we find that lesser the  $Sc$  smaller  $\theta$  and in both types of nanofluids. The values of  $\theta$  and  $C$  in Eg-Cuo nanofluid are relatively greater than those in Eg-Gold nanofluid. Higher  $Sr$  larger  $\theta$  and  $\Phi$  in both types of nanofluids. Figs.15c-15d,  $\theta$  depreciates in the flow region  $(-1,1)$  in  $\gamma > 0$ , in both types of nanofluids, while  $\Phi$  reduces in Eg-Cuo nanofluid, upsurgues in Eg-Gold nanofluid with increase in  $\gamma > 0$ . figs.16c-16d, Increase in  $Q1$  smaller  $\theta$  in  $(-1,0,0.5)$  and larger in the region  $(0,5,1,0)$  in both types of nanofluids.  $\Phi$  decays in Eg-Cuo and Eg-Gold nanofluids with higher values of  $Q1$  in the entire flow region. The values of  $\theta$  in Eg-Cuo nanofluid are smaller than those in Eg-Gold nanofluid while reversed effect is noticed in the values of  $\Phi$  (Figs.17c-17d).

An increase in  $E1$  (Figs.17a-d) depreciates  $\theta$  in the flow region  $(-1,1)$  in both types of nanofluids.  $\Phi$  rises in the flow region  $(-1,0,0.5)$  and decays in  $(0.5,1,0)$  in Eg-Cuo and Eg-Gold nanofluids with higher values of  $E1$ . The values of  $\theta$  in Eg-Cuo nanofluid are relatively greater than those in Eg-Gold nanofluid while values exhibit an opposite behaviour in both types of nanofluids. Higher  $\delta$  larger  $\theta$  and smaller  $\Phi$  in the flow region in both types of nanofluids (fig.18c-18d). The values of  $\theta$  in Eg-Cuo nanofluid are relatively greater than those in Eg-Gold nanofluid, while the values of  $\Phi$  in Eg-Cuo nanofluid are smaller than those in Eg-Gold nanofluid. Increase in index number ( $n$ ) (figs.19c-19d) leads to a decay in temperature and nanoconcentration in both types of nanofluids.

The skin friction components ( $\tau_x, \tau_z$ ), Nusselt and Sherwood number on the boundaries  $\eta = \pm 1$  are shown in table.3a & 3b for different parametric variations in Eg-Cuo and Gold nanofluids. The skin friction component ( $\tau_x$ ) upsurgues at  $\eta = \pm 1$  with rising values of Grashof number ( $G$ )/rotation parameter ( $R$ )/radiation parameter ( $Rd$ )/Eckert number ( $Ec$ ) in Eg based CuO nanofluid and Eg-Gold nanofluid.  $\tau_x$  reduces with porous parameter ( $K$ )/nanoparticle volume fraction ( $\phi$ ) at both the walls in Eg-Cuo and Gold nanofluid. Increase in magnetic parameter ( $M$ ) enhances  $\tau_x$  in Eg-Cuo nanofluid and reduces in Eg-Gold nanofluid at  $\eta = \pm 1$ .  $\tau_x$  reduces in Eg-Cuo nanofluid and enhances in Eg-Gold nanofluid at  $\eta = \pm 1$  with rising values of Hall parameter ( $m$ )/heat generating/absorbing source ( $0 < Q < 0$ )/Prandtl number ( $Pr$ ).

The skin friction component ( $\tau_x$ ) augments at both walls, while  $\tau_z$  enhances at left wall and reduces at the right wall with higher values of  $G/Ec$  in Eg based CuO nanofluid Increase in  $M/m/R/Rd$  reduces  $\tau_x$ , enhances  $\tau_z$  at  $\eta = \pm 1$  in Eg-Cuo nanofluid. Higher the  $K/Q/Pr$  decays at both walls in Eg-Cuo nanofluid. In the case of Eg based Gold nanofluid,  $\tau_x$  and  $\tau_z$  grows at the both walls with increasing values of  $Rd/Ec/Q/Pr$  while they decay with  $M$ . Higher the  $m$  reduces  $\tau_x$  at the left wall, enhances at the

right wall while  $\tau_z$  enhances at both the walls. Increase in  $R$  reduces  $\tau_x$  and enhances  $\tau_z$  at both the walls.  $\tau_x$  enhances at  $\eta=-1$ , reduces at  $\eta=+1$  and  $\tau_z$ , grows at both the walls with higher values of  $s$ . An upsurge in  $\phi$  grows  $\tau_x$ , decays  $\tau_z$  at both the walls in Eg-Gold nanofluid. Higher the thermal buoyancy force ( $G$ ) larger  $\tau_x$  at the left wall, decays at the right wall while  $\tau_z$  exhibit an opposite behaviour at the wall with  $G$  in Eg-Gold nanofluid (table.3a &3b).

The rate of heat transfer(Nusselt number) at  $\eta=\pm 1$  decays at the left wall and enhances at the right wall with increasing values of  $G/M/Rd/ Ec/\phi/Sr/Q1$  in Eg based Cuo nanofluid while in Eg-Gold nanofluid,  $Nu$  reduces at  $\eta=-1$  and enhances at enhances with rising values of  $m$  in Eg-Cu and Gold nanofluids.  $Nu$  reduces at  $\eta=-1$ ,grows at  $\eta=+1$  with increasing values of  $G/M/ Ec/Q1/\delta$ . $Nu$  enhances at  $\eta=-1$  and decays at  $\eta=+1$ ,in Eg based Cuo nanofluid with increase in  $m/K/Q/Pr/\gamma/Sc/n$  while in Eg-Gold nanofluid, it behaves in the same manner with  $S/Rd/Q/\phi/Sc/\gamma$  at the walls.  $Nu$  reduces at  $\eta=\pm 1$  with  $E1$  in Eg-Cuo nanofluid while in Eg based Gold nanofluid it exhibit in the same manner with higher values of  $S/Rd/Q/\phi/Sc/\gamma$ .  $Nu$  enhances at  $\eta=\pm 1$  with larger values of  $m/Pr/Sr$  in Eg based Gold nanofluid.

The rate of mass transfer(Sherwood number) at  $\eta=\pm 1$  shows that increase in  $G/ M/R/\gamma$  in Eg based Gold nanofluid while in Eg-Cuo nanofluid,  $Sh$  enhances with higher values of  $m/Q1$  leads to an enhancement at both the walls,  $Sh$  enhances at the left wall and reduces at the right wall with increase in  $G/R/ Ec/\phi/Sc/\gamma/\delta/n$  in Eg based Cuo nanofluid while in Eg-Gold nanofluid, it behaves in the same manner with higher values of  $m/S/Rd/ Ec/Sc/Q1/E1/n$ . Increase in  $M/K/q/Pr/Rd/Sr/E1$  reduces  $Sh$  at  $\eta=-1$  and enhances at  $\eta=+1$  in Eg based Cuo nanofluid while in Eg-Gold nanofluid,  $Sh$  exhibit the same behaviour with larger values of  $Q/\phi/Pr/Sr/\delta$ (table.3a &3b).

## 6. CONCLUSIONS:

The effect of activation, Hall effect, thermo-diffusion and heat sources on the hydromagnetic flow of Eg based Cuo and Gold nanofluids in a vertical channel has been analysed by using by numerical method. The important findings of this analysis are:

- 1) Increase in  $G/Rd/ Ec$  enhances both  $u,w$ .  $\theta$  upsurgs,  $\Phi$  decays in the flow region.
- 2) Increase in  $M/R$  decays  $u$  and grows the  $w$ .  $\theta$  upsurgs,  $\Phi$  decays in the flow region.
- 3) Higher  $K$  smaller  $u$  and  $\Phi$ .  $w$  and  $\theta$  reduces in the region(-1,0.5) and enhances in the region(0.5,1,0) with rising values of  $K$ .
- 3)  $u$ ,  $\Phi$  reduces in Eg-Cuo nanofluid while they enhance in Eg-Gold nanofluid.  $w$  and  $\theta$  grow in Eg-Cuo nanofluid and reduces in Eg-Gold nanofluid with higher values of  $m$
- 4) Higher  $Rd/ Ec$  larger  $u,w$  both types of nanofluids.  $\theta$  upsurgs,  $\Phi$  decays in the flow region.
- 5)  $u,w$  decays in both types of nanofluids with larger values of  $\phi/Pr$ .
- 6)  $\theta$  and  $\Phi$  depreciate with  $Sc/Q1$  and grows with  $Sr$  in the flow region in both types of nanofluids. Higher the activation energy parameter( $E1$ ) smaller the temperature and larger the nanoconcentration in the flow region.
- 7) In all the variations, the values of  $u$ ,  $\Phi$  in Eg-Cuo nanofluid are lesser than those in Eg-Gold nanofluid with increase in  $R$ .
- 8) The values of  $u,w,C$  in Eg-Cuo nanofluid are relatively greater than those in Eg-Gold nanofluid while the values of  $\theta$  in Eg-Cuo nanofluid are smaller than those in Eg-Gold nanofluid.
- 9) The values of  $u,w,\theta$  in Eg-Cuo nanofluid are lesser than those in Eg-Gold nanofluid while values of  $C$  in Eg-Cuo nanofluid are greater than those in Eg-Gold nanofluid.
- 10) The values of  $u,w,\theta$  and  $C$  in Eg-Cuo nanofluid are greater than those in Eg-Gold nanofluid with higher values of nanoparticle volume fraction ( $\phi$ ).
- 11) With respect to variation of Activation energy parameter( $E1$ ),we find that the values of  $\theta$  in Eg-Cuo nanofluid are greater than those in Eg based Gold nanofluid, while opposite behaviour is noticed on the values of  $\Phi$  in the flow region.
- 12) Increase in  $R$  reduces  $\tau_x$  and enhances  $\tau_z$  in both types of nanofluids.
- 13) An increase in  $\phi$  upsurgs  $\tau_x$  and decays  $\tau_z$  at both the walls.
- 14)  $Nu$  enhances at left wall and reduces at the right wall in Eg-Cuo nanofluid with rising values of  $m/Q/\gamma$  while in Eg-Gold nanofluid, it exhibit the same behavior with higher values of  $Rd/Q/\phi/Sc/\gamma$ . $Nu$  reduces at both the walls with larger values of  $E1$  at  $\eta=\pm 1$ .
- 15) The  $Sh$  grows with  $m/Q1$  in Eg-Cuo nanofluid while in Eg-Gold nanofluid, it upsurgs with  $G/M/R/\gamma$ .
- 16)  $Sh$  decays at  $\eta=-1$  and grows at  $\eta=+1$  with increase in  $M/K/Q/Rd/Se/E1$  in Eg based Cuo nanofluid while in Eg-Gold nanofluid,  $Sh$  exhibits the same nature with  $Q/\phi/Sr/Pr/\delta$ .

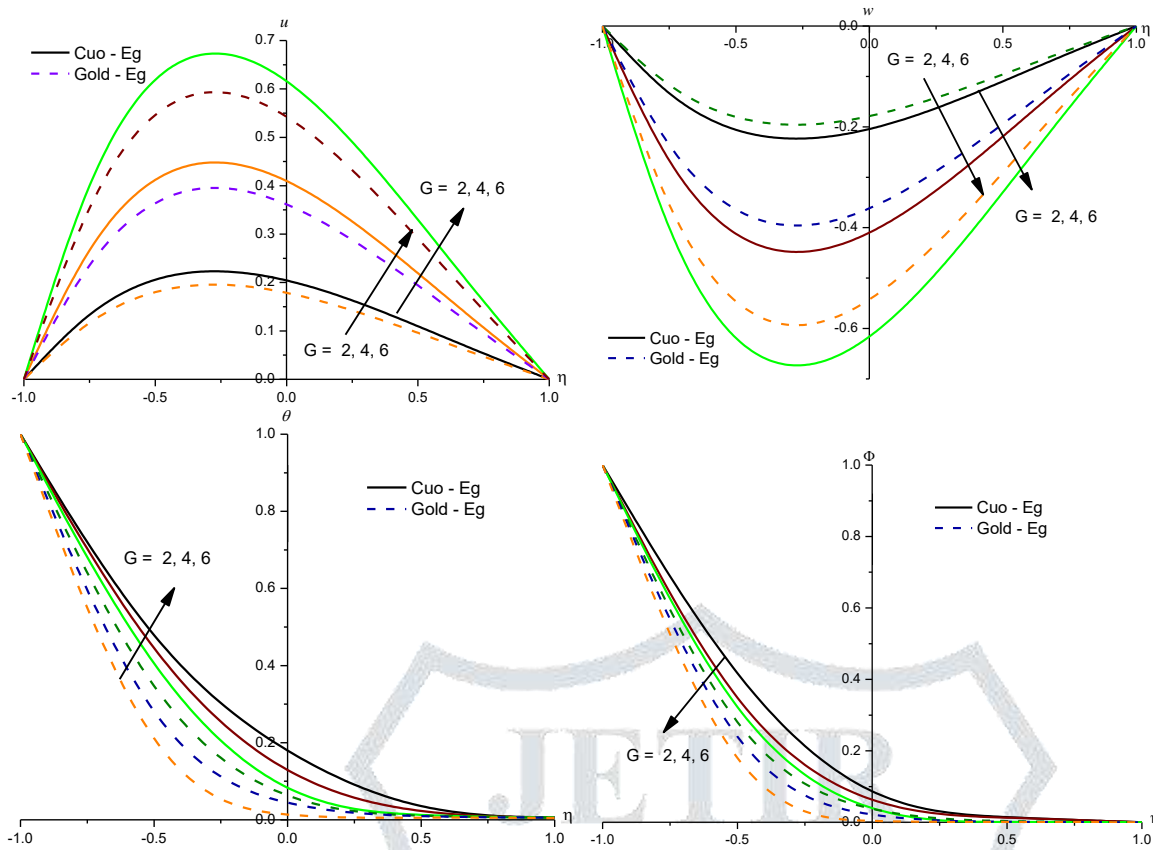


Fig.2 : Variation of [a] Axial velocity ( $u$ ), [b] Secondary velocity( $w$ ), [c] Temperature( $\theta$ ), [d] Nanoconcentration( $\Phi$ ) with  $G$   
 $M=0.5, m=0.25, K=0.3, s=0.1, R=0.5, Rd=0.5, Ec=0.1, Q=0.5, \phi=0.1, Pr=0.2, Sc=0.24, Sr=0.5, \gamma=0.5, Q1=0.25, E1=0.1, \delta=0.2, n=0.2$

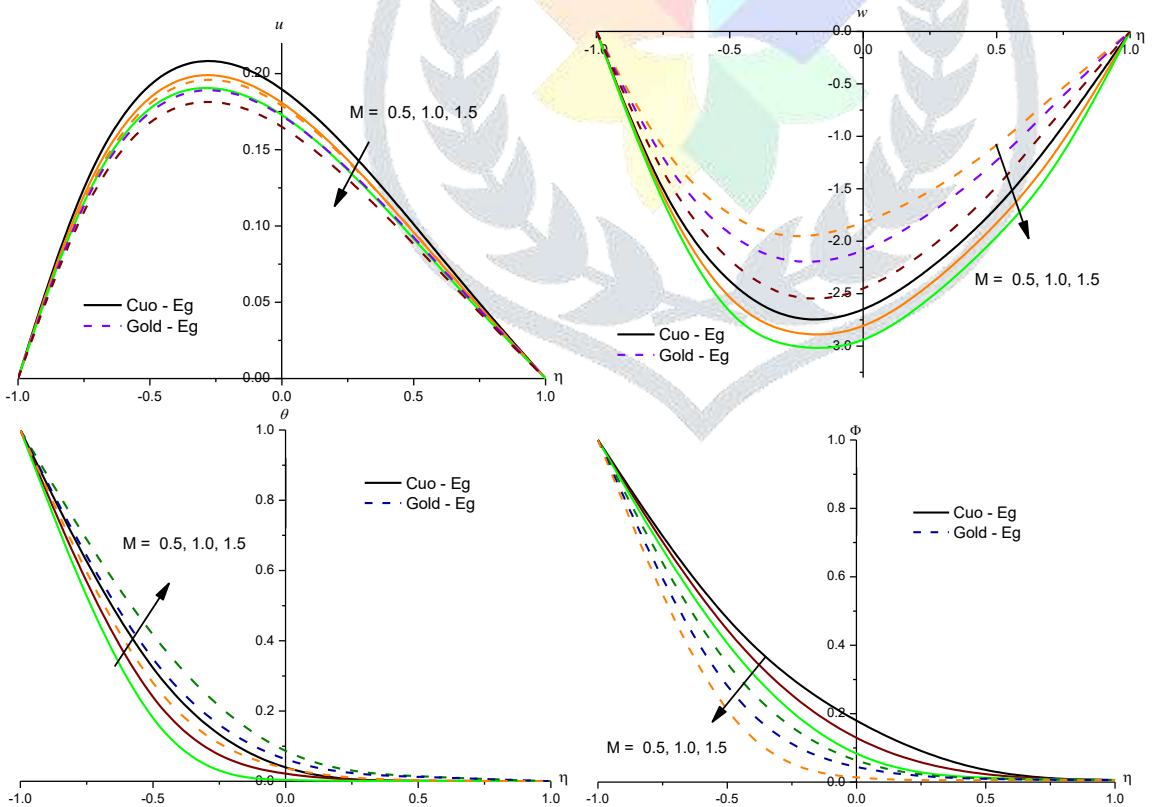


Fig.3 : Impact of  $M$  on  $u, w, \theta$  and  $\Phi$

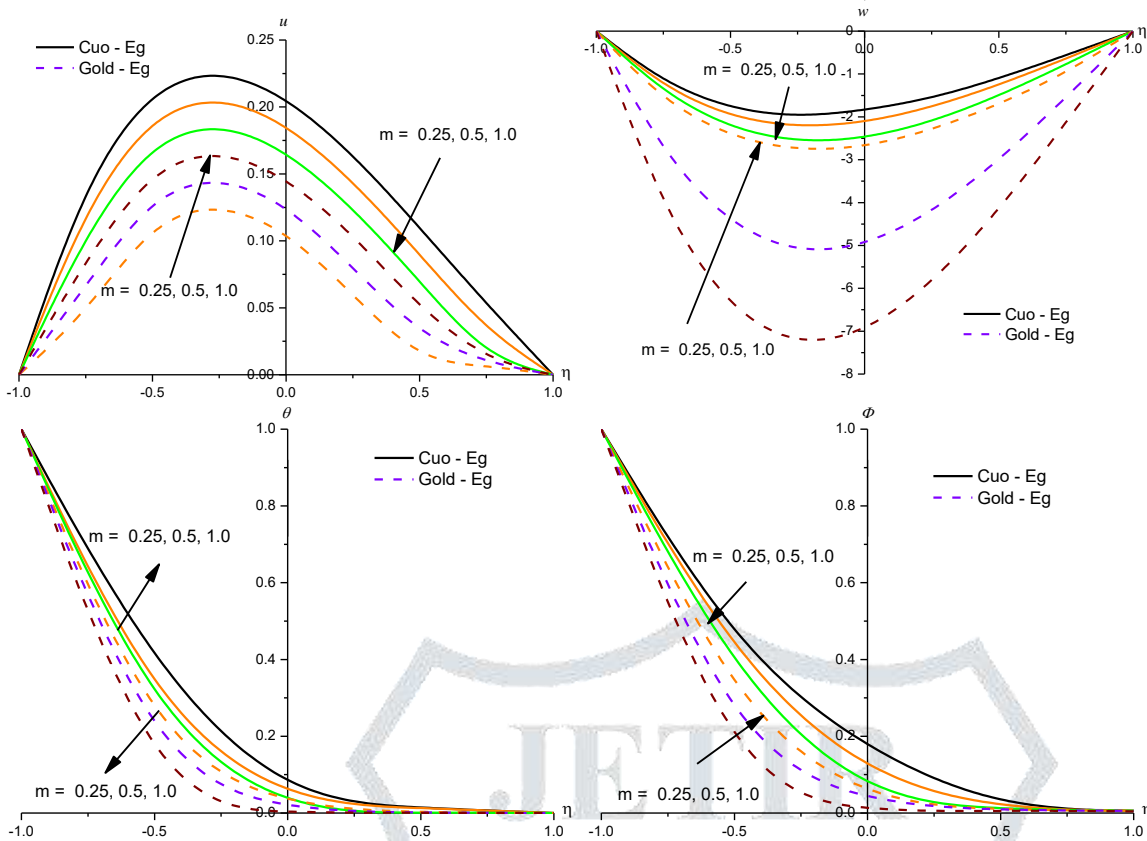


Fig.4 : Impact of  $m$  on  $u, w, \theta$  and  $\Phi$

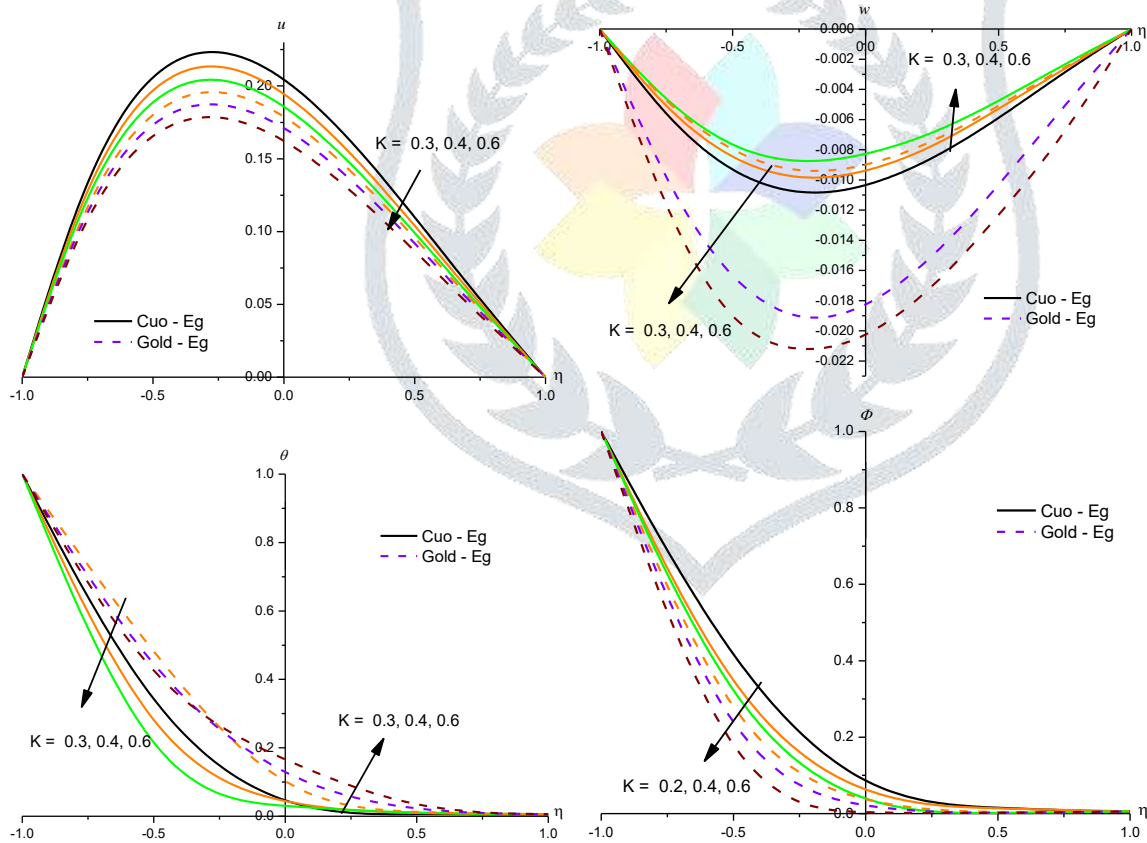


Fig.5 : Impact of  $K$  on  $u, w, \theta$  and  $\Phi$

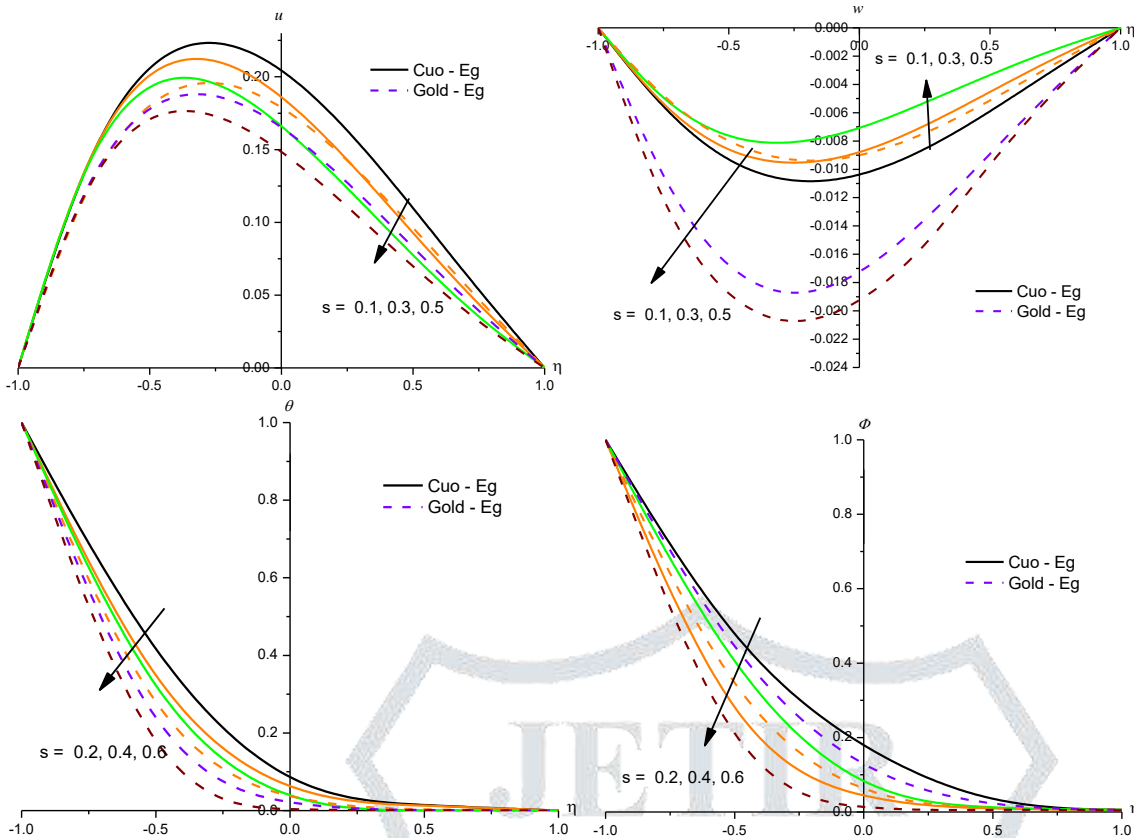


Fig.6 : Impact of s on u, w,  $\theta$  and  $\Phi$

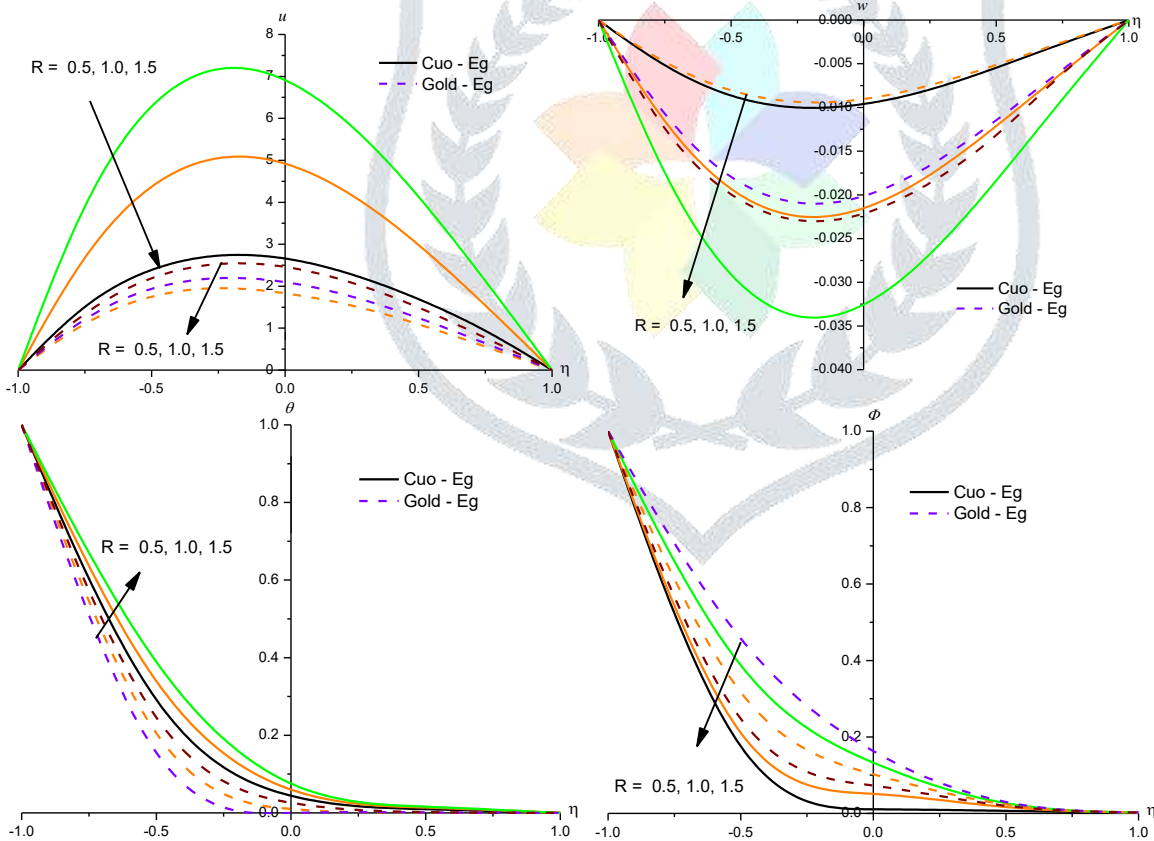


Fig.7 : Impact of R on u, w,  $\theta$  and  $\Phi$

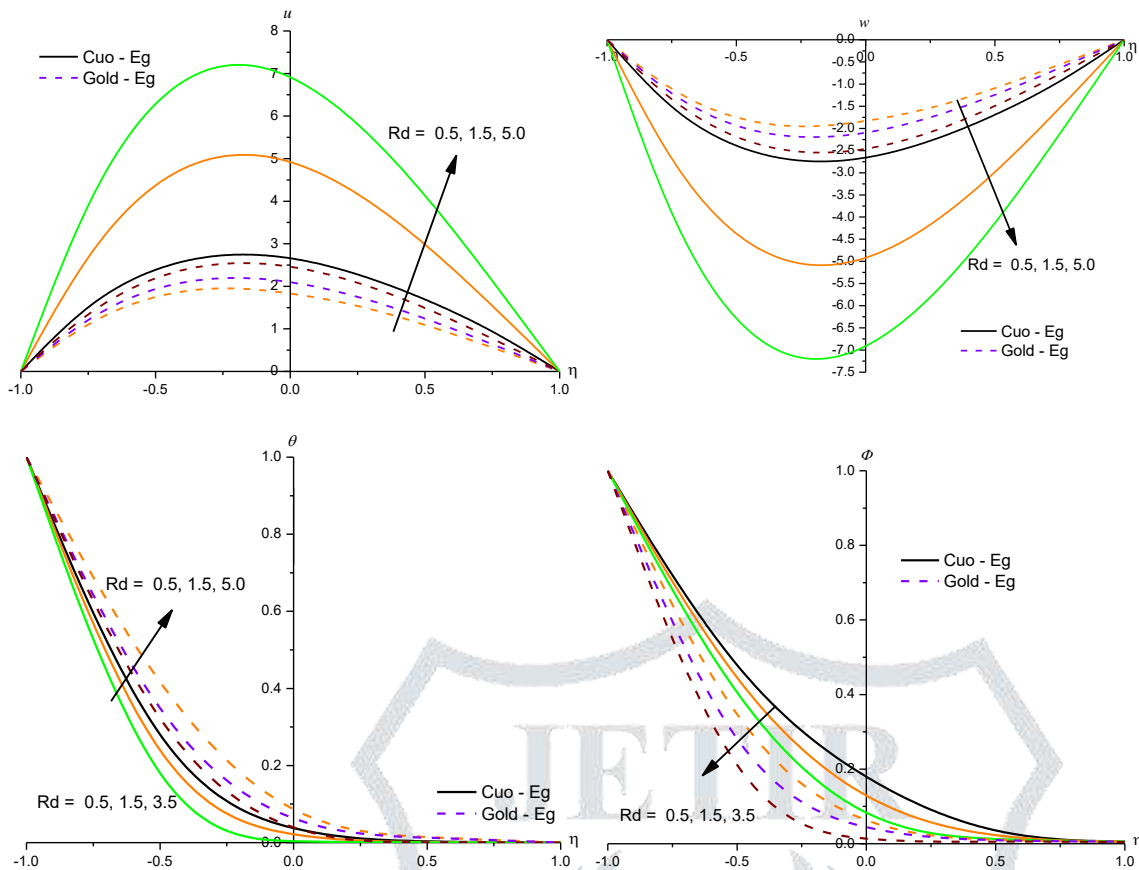


Fig.8 : Impact of  $Rd$  on  $u$ ,  $w$ ,  $\theta$  and  $\Phi$

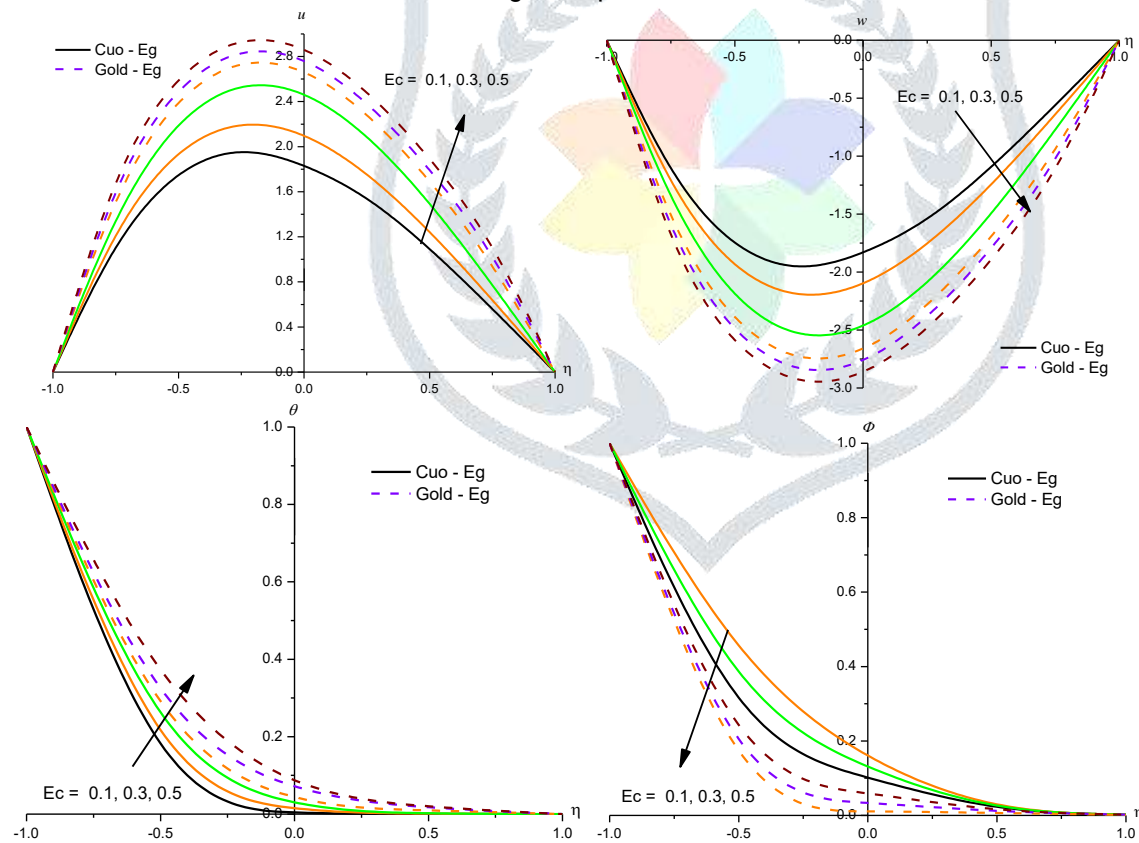


Fig.9 : Impact of  $Ec$  on  $u$ ,  $w$ ,  $\theta$  and  $\Phi$

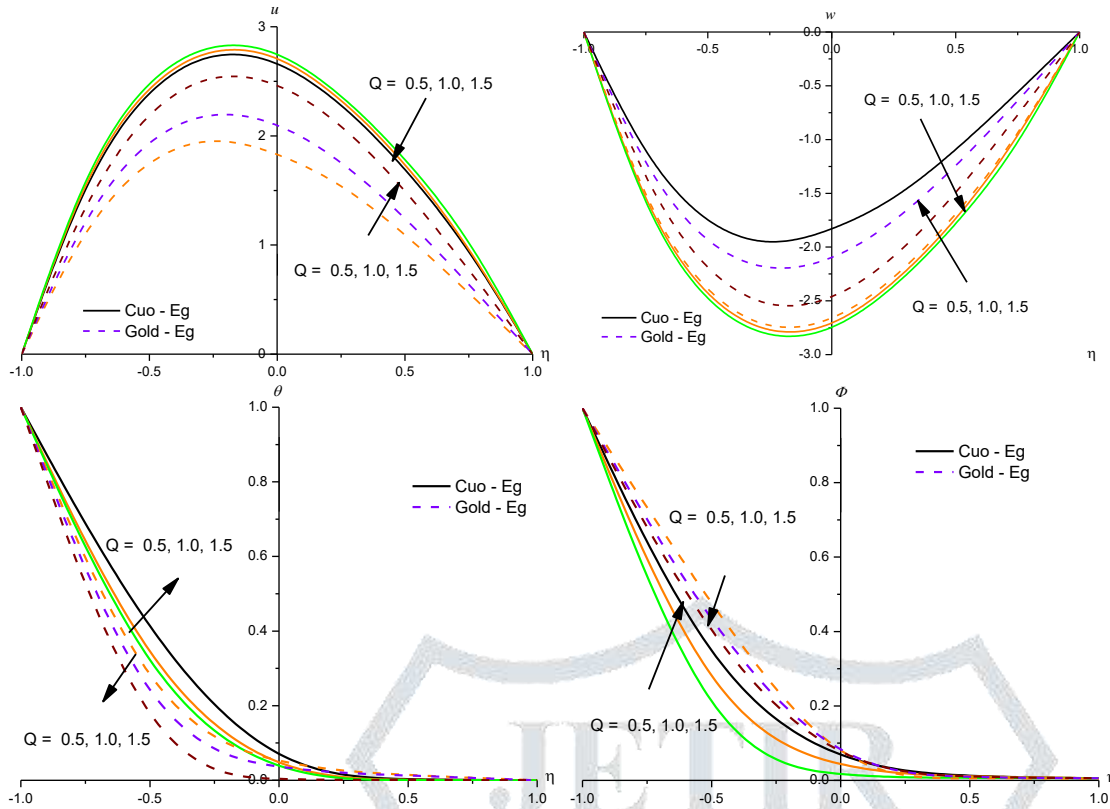


Fig.10 : Impact of  $Q$  on  $u, w, \theta$  and  $\Phi$

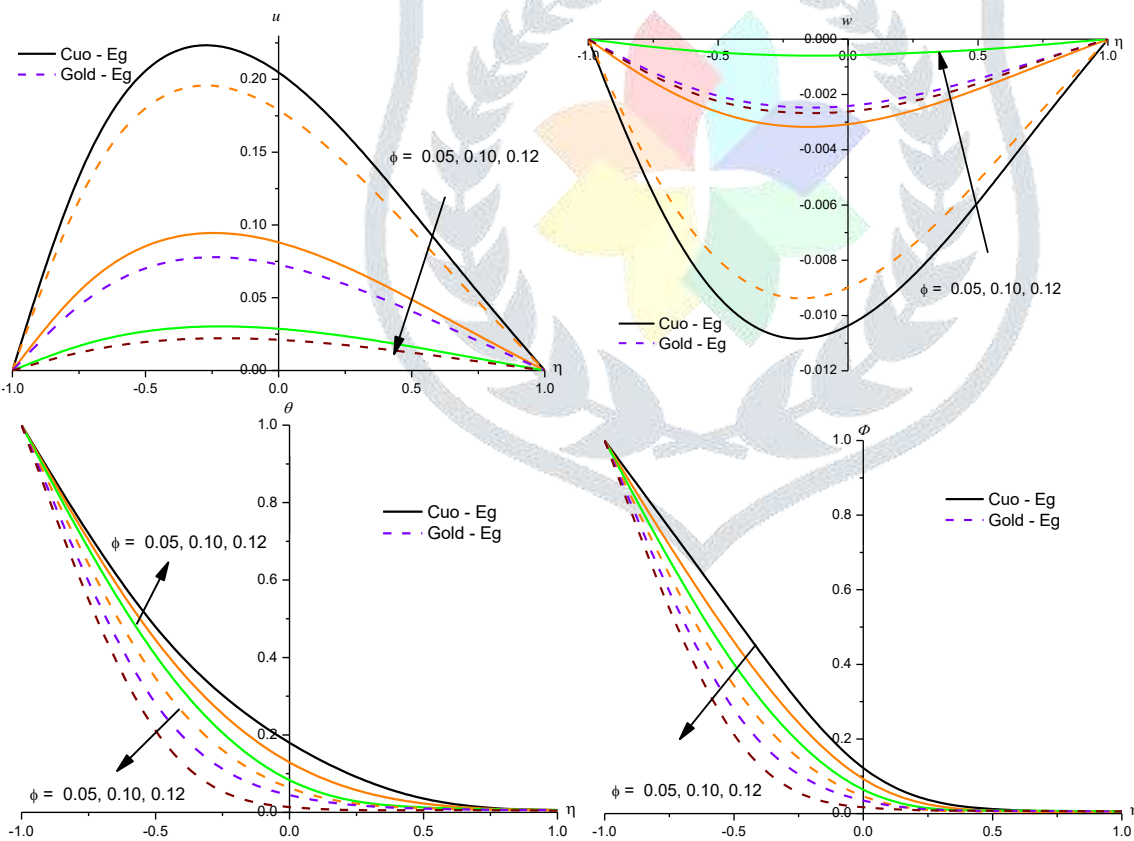


Fig.11 : Impact of  $\phi$  on  $u, w, \theta$  and  $\Phi$

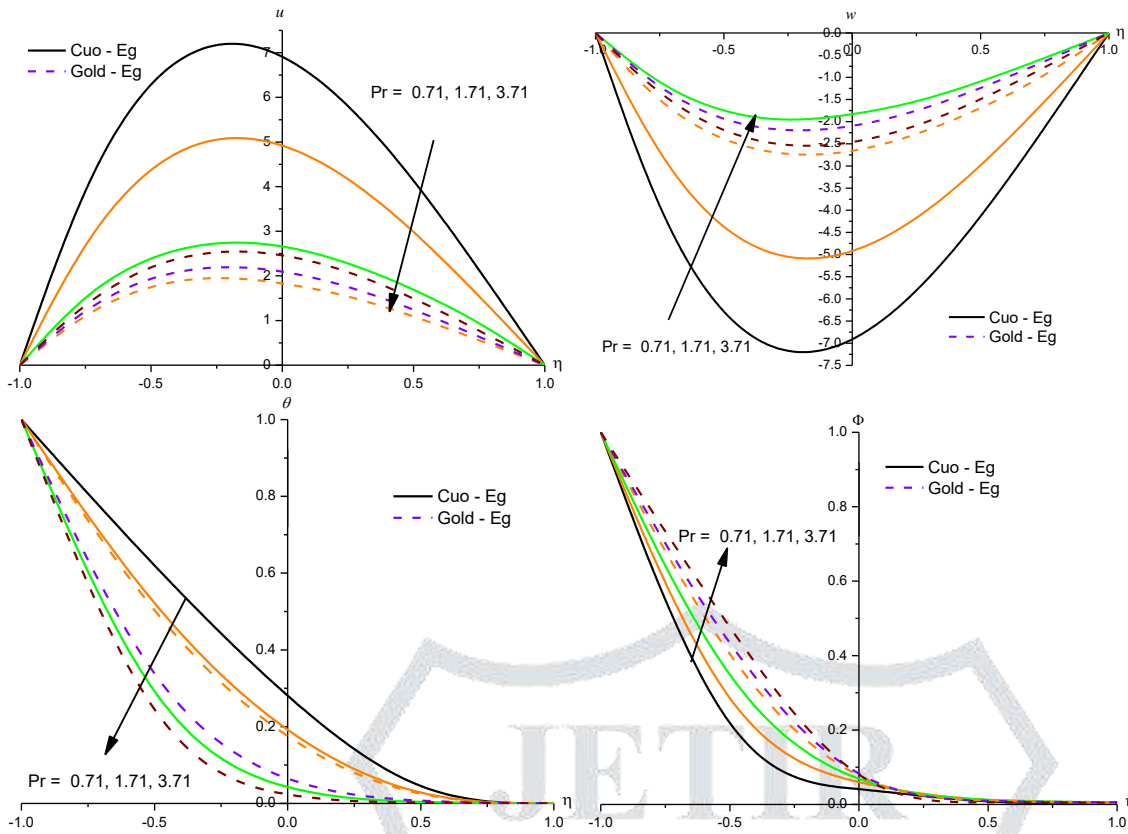


Fig.12 : Impact of Pr on u, w,  $\theta$  and  $\Phi$

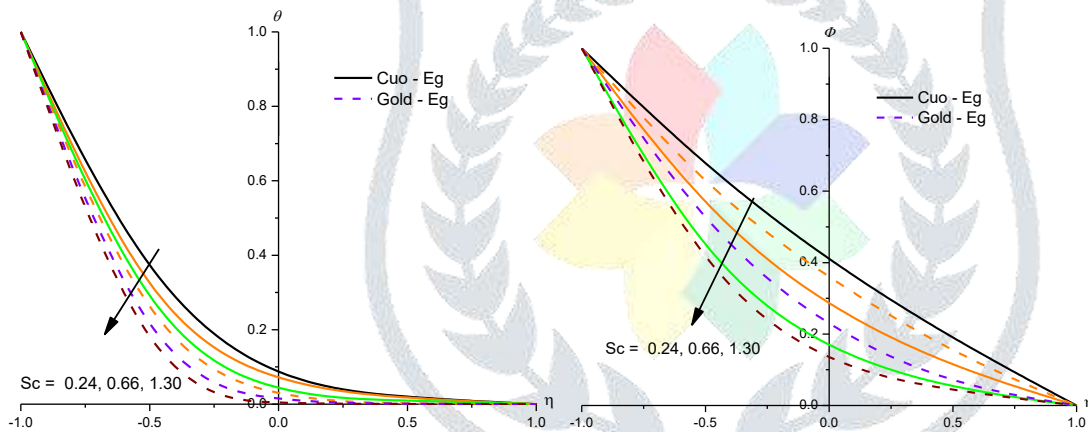


Fig.13 : Impact of Sc on  $\theta$  and  $\Phi$

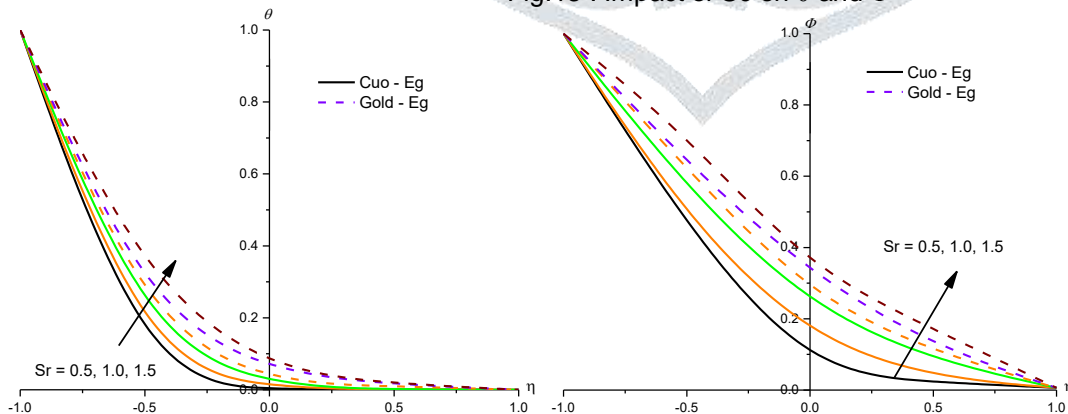


Fig.14 : Impact of Sr on  $\theta$  and  $\Phi$

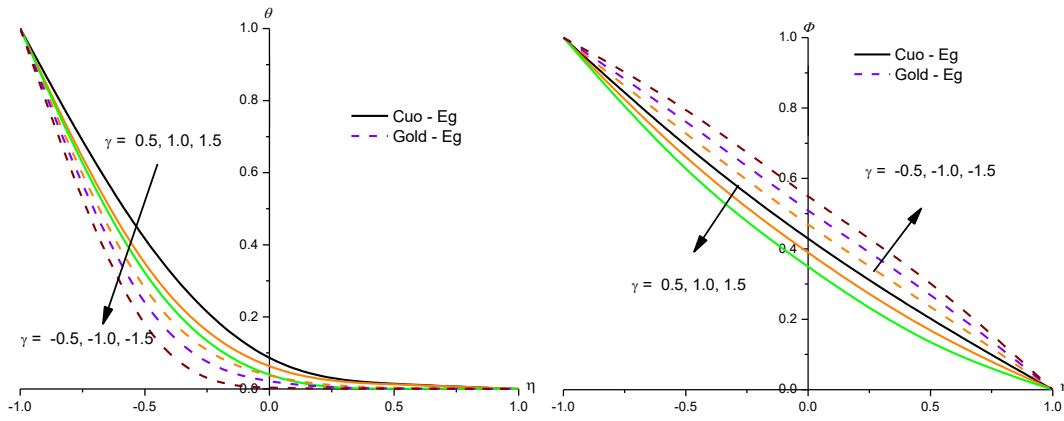


Fig.15 : Impact of  $\gamma$  on  $\theta$  and  $\Phi$

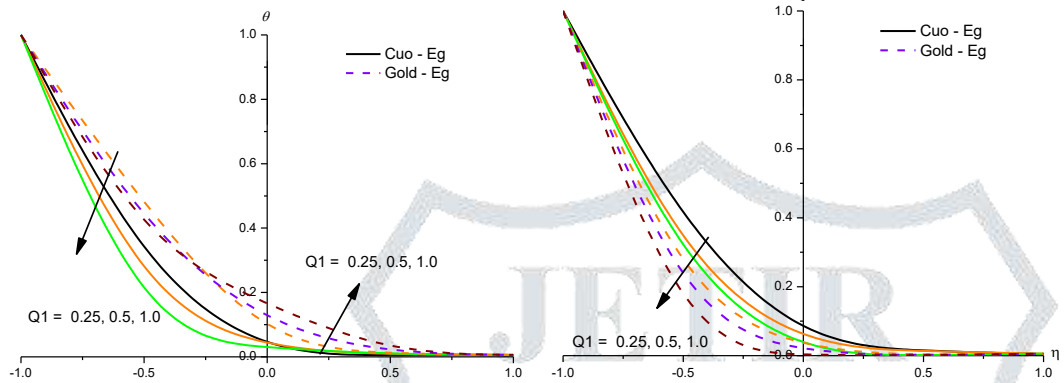


Fig.16 : Impact of  $Q1$  on  $\theta$  and  $\Phi$

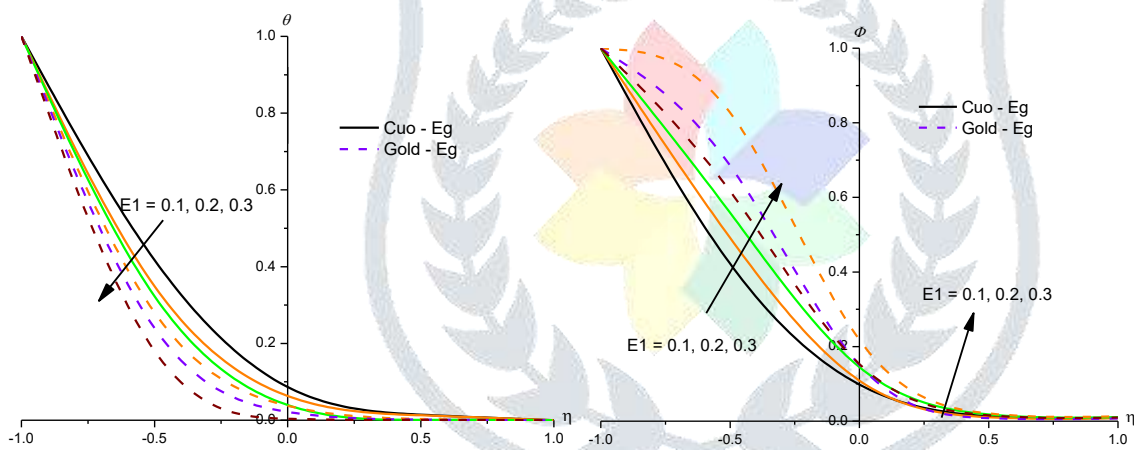


Fig.17 : Impact of  $E1$  on  $\theta$  and  $\Phi$

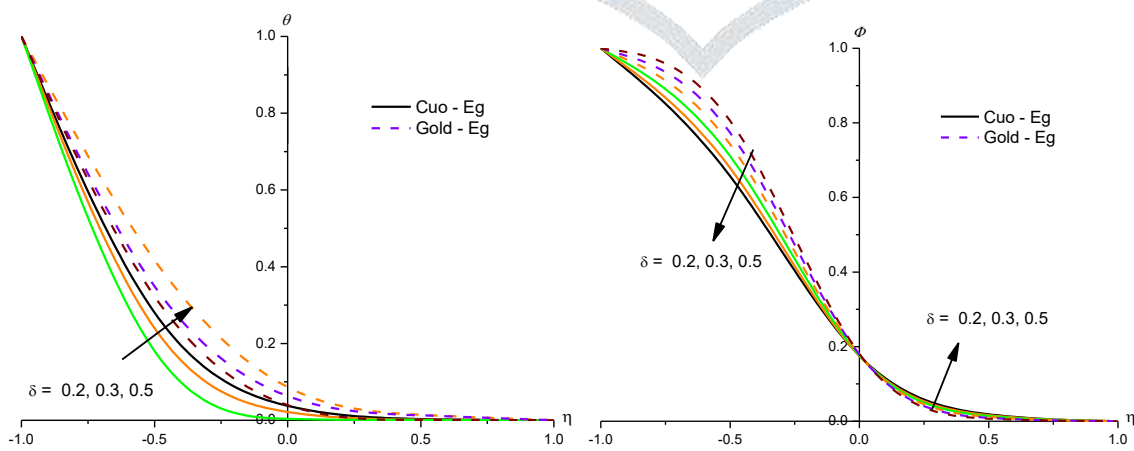


Fig.18 : Impact of  $\delta$  on  $\theta$  and  $\Phi$

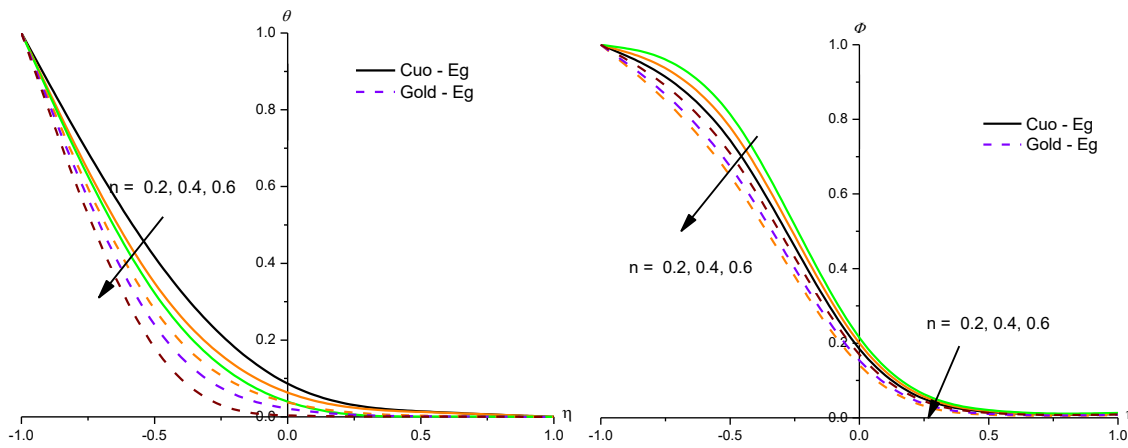


Fig.19 : Impact of  $n$  on  $\theta$  and  $\Phi$

Table 3a: Skin friction components( $\tau_x, \tau_z$ )at  $\eta = \pm 1$

Parameters		Eg-Cuo-nanofluid				Eg-Gold nanofluid			
		$\tau_x(-1)$	$\tau_x(+1)$	$\tau_z(-1)$	$\tau_z(+1)$	$\tau_x(-1)$	$\tau_x(+1)$	$\tau_z(-1)$	$\tau_z(+1)$
G	2	0.774688	-0.194917	-0.0273761	0.5423885	0.682837	-0.171903	-0.0234494	0.5104154
	4	1.549644	-0.389953	-0.0547656	0.5421125	1.378096	-0.346942	-0.0473259	0.5103574
	6	2.328353	-0.586753	-0.0823387	0.5354045	2.067246	-0.520463	-0.0709945	0.5102694
M	0.5	0.734333	-0.179382	-0.0254672	0.0098273	0.682837	-0.171903	-0.0234494	0.2281794
	1.0	0.712043	-0.170903	-0.0386945	0.0149439	0.667963	-0.165241	-0.0361606	0.0143254
	1.5	0.690537	-0.162828	-0.0536632	0.0207593	0.647586	-0.157383	-0.0502985	0.0199584
R	0.5	0.734333	-0.179382	-0.0254672	0.0098273	0.682837	-0.171903	-0.0234494	0.0092817
	1.0	0.730973	-0.177971	-0.0568281	0.0219125	0.686013	-0.172166	-0.0524722	0.0207551
	1.5	0.724792	-0.175382	-0.0858058	0.0330399	0.690387	-0.189746	-0.0791177	0.0312526
m	0.25	0.774688	-0.194917	-0.0273761	0.0106344	0.682837	-0.171903	-0.0234494	0.0092817
	0.5	0.770075	-0.193123	-0.0291402	0.0112996	0.692762	-0.174934	-0.0256167	0.0101366
	1.0	0.767035	-0.191951	-0.0293524	0.0113713	0.691433	-0.175987	-0.0260764	0.0103209
S	0.1	0.774688	-0.194917	-0.0273761	0.0106367	0.682837	-0.171903	-0.0234494	0.0092817
	0.3	0.821854	-0.149557	-0.0280647	0.0073107	0.729822	-0.134911	-0.0543017	0.0146046
	0.5	0.859642	-0.113917	-0.0297297	0.0048655	0.761653	-0.104023	-0.0820867	0.0150571
K	0.3	0.774688	-0.194917	-0.0273761	0.0106355	0.682837	-0.171903	-0.0234494	0.0092817
	0.4	0.748248	-0.184697	-0.0249241	0.0095983	0.664673	-0.163829	-0.0478951	0.0188116
	0.6	0.724663	-0.175662	-0.0228426	0.0087255	0.641102	-0.154525	-0.0666068	0.0258871
Rd	0.5	0.774688	-0.194917	-0.0273761	0.0106367	0.682837	-0.171903	-0.0234494	0.0092817
	1.5	0.783668	-0.199045	-0.0278292	0.0108295	0.687918	-0.173064	-0.0526838	0.0208506
	5.0	0.782876	0.205306	-0.0279407	0.0108786	0.692716	-0.174846	-0.0795124	0.0314314
Ec	0.1	0.774688	-0.194917	-0.0273761	0.0106367	0.682837	-0.171903	-0.0234494	0.0928179
	0.3	0.774709	-0.194927	-0.0273772	0.0106305	0.686017	-0.172167	-0.0524726	0.1020755
	0.5	0.774967	-0.195048	-0.0273898	0.0106261	0.690393	-0.173979	-0.0791184	0.0312532
Q	0.5	0.774688	-0.194917	-0.0273761	0.0106356	0.682837	-0.171903	-0.0234494	0.0092879
	1.0	0.761845	-0.189208	-0.0267354	0.0103501	0.683234	-0.170896	-0.0521666	0.0206183
	1.5	0.749666	-0.183829	-0.0261286	0.0100858	0.674928	-0.167253	-0.0782018	0.0308443
$\phi$	0.05	0.774688	-0.194917	-0.0273761	0.0106367	0.682837	-0.171903	-0.0234494	0.0092816
	0.10	0.307996	-0.090518	-0.0073847	0.0034311	0.751236	-0.176434	-0.0056781	0.0027653
	0.12	0.093789	-0.031611	-0.0014638	0.00079925	0.067179	-0.024087	-0.0009158	0.0005371
Pr	0.71	0.787912	-0.200995	-0.0280436	0.0109245	0.685626	-0.173216	-0.0235886	0.0093443
	1.71	0.785501	-0.199883	-0.0279217	0.0108703	0.691327	-0.174547	-0.0237766	0.0094176
	3.71	0.774807	-0.194973	-0.0273819	0.0106326	0.693024	-0.175461	-0.0239619	0.0098658

Table 3b : Nusselt and Sherwood number( $Nu, Sh$ )at  $\eta = \pm 1$

Parameters		Eg-Cu o-nanofluid				Eg-Gold nanofluid			
		$Nu(-1)$	$Nu(+1)$	$Sh(-1)$	$Sh(+1)$	$Nu(-1)$	$Nu(+1)$	$Sh(-1)$	$Sh(+1)$
G	2	0.542388	0.476204	0.691196	0.366828	0.51041	0.494039	0.695191	0.364984
	4	0.542112	0.476392	0.691231	0.366809	0.510357	0.494076	0.695198	0.364988
	6	0.535404	0.479052	0.692055	0.366525	0.510269	0.494136	0.695209	0.364994
M	0.5	0.542401	0.476195	0.691194	0.366829	0.510416	0.494039	0.695191	0.364984
	1.0	0.542375	0.476215	0.691178	0.366819	0.510403	0.494044	0.695192	0.364988
	1.5	0.541826	0.476414	0.691265	0.366825	0.510399	0.494047	0.695195	0.364991
R	0.5	0.542401	0.476195	0.691194	0.366829	0.51041	0.494039	0.695191	0.364984
	1.0	0.542381	0.476194	0.691196	0.366822	0.51042	0.494044	0.695193	0.364986
	1.5	0.541804	0.476013	0.691268	0.366806	0.51045	0.494049	0.695199	0.364989
m	0.25	0.542388	0.476204	0.691196	0.366828	0.51041	0.494039	0.695191	0.364984
	0.5	0.542396	0.476202	0.691199	0.366829	0.51045	0.494044	0.695195	0.364983
	1.0	0.542716	0.476154	0.691278	0.366901	0.51049	0.494049	0.695199	0.364980
K	0.3	0.542388	0.476204	0.691196	0.366828	0.51041	0.494039	0.695191	0.364984
	0.4	0.542396	0.476198	0.691195	0.366829	0.510412	0.494038	0.695193	0.364988

Parameters	Eg-Cu o-nanofluid				Eg-Gold nanofluid				
		Nu(-1)	Nu(+1)	Sh(-1)	Sh(+1)	Nu(-1)	Nu(+1)	Sh(-1)	Sh(+1)
S	0.6	0.542417	0.476006	0.691066	0.366837	0.510413	0.494037	0.695196	0.364992
	0.1	0.542388	0.476204	0.691196	0.366828	0.510415	0.494039	0.695191	0.364984
	0.3	0.545487	0.476278	0.761892	0.322049	0.511194	0.493268	0.766298	0.320092
	0.5	0.547921	0.470543	0.836982	0.281496	0.511979	0.492498	0.841732	0.279462
Rd	0.5	0.542388	0.476204	0.691196	0.366828	0.510416	0.494039	0.695191	0.364984
	1.5	0.516441	0.490667	0.694437	0.365332	0.504012	0.497696	0.695991	0.364605
	5.0	0.510027	0.494261	0.695239	0.364967	0.502485	0.498572	0.696182	0.364514
Ec	0.1	0.542388	0.476204	0.691196	0.366828	0.510415	0.494039	0.695191	0.364984
	0.3	0.542342	0.476235	0.691202	0.366825	0.510401	0.494046	0.695192	0.364983
	0.5	0.540921	0.476782	0.691376	0.366767	0.510393	0.494051	0.695193	0.364982
Q	0.5	0.542388	0.476204	0.691196	0.366828	0.510441	0.494039	0.695191	0.364987
	1.0	0.581456	0.457577	0.686328	0.368728	0.520158	0.489222	0.693975	0.365065
	1.5	0.618725	0.440173	0.681685	0.370499	0.529831	0.484469	0.692769	0.3651236
$\phi$	0.05	0.542388	0.476204	0.691196	0.366828	0.510416	0.494039	0.695191	0.364984
	0.10	0.542201	0.476402	0.691225	0.366807	0.510453	0.494001	0.695185	0.364988
	0.12	0.541965	0.476624	0.691249	0.366783	0.510482	0.493974	0.695182	0.364991
Pr	0.71	0.504291	0.497551	0.695956	0.364623	0.501044	0.499467	0.696362	0.364428
	1.71	0.511188	0.493635	0.695094	0.365025	0.502727	0.498434	0.696151	0.364528
	3.71	0.541697	0.476463	0.691281	0.366801	0.510414	0.504046	0.695191	0.364984
Sc	0.24	0.542388	0.476204	0.691196	0.366828	0.510414	0.494039	0.695091	0.364989
	0.66	0.542911	0.475766	1.055984	0.206286	0.510545	0.493934	1.067641	0.202395
	1.30	0.543855	0.475606	1.592865	0.090335	0.511684	0.493625	1.615284	0.085407
Sr	0.5	0.542388	0.476204	0.691196	0.366828	0.510414	0.494039	0.695191	0.364984
	1.0	0.542384	0.476207	0.688573	0.368048	0.510437	0.494044	0.694546	0.365289
	1.5	0.541689	0.476469	0.686171	0.369187	0.510488	0.494049	0.693915	0.365589
$\gamma$	0.5	0.542388	0.476204	0.691196	0.366828	0.510414	0.494039	0.695191	0.364984
	1.0	0.542434	0.476167	0.723438	0.355039	0.510421	0.494035	0.727455	0.353221
	1.5	0.543786	0.476091	0.754357	0.343963	0.510432	0.494022	0.758204	0.358198
Q1	0.25	0.542388	0.476204	0.691196	0.365789	0.510414	0.494039	0.695191	0.364984
	0.5	0.540535	0.477039	0.691427	0.376799	0.509967	0.494246	0.695247	0.364963
	1.0	0.53836	0.477968	0.691696	0.380786	0.509678	0.494414	0.695292	0.364946
E1	0.1	0.542388	0.476204	0.691196	0.366828	0.510417	0.494039	0.695191	0.364984
	0.2	0.542372	0.476217	0.679761	0.371255	0.510406	0.494043	0.683783	0.369388
	0.3	0.541668	0.476187	0.671122	0.374588	0.510403	0.494045	0.675076	0.372742
$\delta$	0.2	0.542388	0.476204	0.691196	0.366828	0.510413	0.494039	0.695191	0.364984
	0.3	0.542393	0.476256	0.694738	0.365934	0.510411	0.494036	0.698763	0.364074
	0.5	0.541705	0.476459	0.697844	0.365136	0.510402	0.494032	0.701805	0.363293
n	0.2	0.542388	0.476204	0.691196	0.366828	0.510413	0.494039	0.695191	0.364984
	0.4	0.542391	0.476202	0.693281	0.366321	0.510411	0.494037	0.697296	0.364467
	0.6	0.541702	0.476159	0.695259	0.365832	0.510410	0.494033	0.699207	0.363998

## 7. REFERENCES

- [1]. Abolbashari, Mohammad Hossein, Navid Freidoonimehr, Foad Nazari, and Mohammad Mehdi Rashidi. "Entropy analysis for an unsteady MHD flow past a stretching permeable surface in nano-fluid." *Powder Technology* 267 (2014): 256-267. <https://doi.org/10.1016/j.powtec.2014.07.028>
- [2]. Arundhati V, Chandra Sekhar K.V., Prasada Rao D.R.V., Sreedevi G : Thermal Radiation and Thermodiffusion Effect on Convective Heat and Mass Transfer Flow of a Rotating Nanofluid in a Vertical Channel, *International Conference on Numerical Heat Transfer & Fluid Flow* (NHTFF18), National Institute of Technology (NIT) Warangal, TS, India on Jan 19-21, (2018); *Numerical Heat Transfer and Fluid Flow*: Select Proceedings of NHTFF 2018 (Springer) pp.73-81. [https://DOI.org/10.1007/978-981-13-1903-7\\_10](https://DOI.org/10.1007/978-981-13-1903-7_10)
- [3]. Baker, David H. (1999). "Cupric Oxide Should Not be Used as a Copper Supplement for Either Animals or Humans". *The Journal of Nutrition*. 129 (12): 2278–2279. doi:10.1093/jn/129.12.2278. PMID 10573563.
- [4]. Bentoto W, Zaydan M., Amini Alaoui H., Essaghir E. and Sehaqui R. : Mixed convection of a MHD oscillatory laminar flow of a nanofluid (Gold-Kerosene oil) in a vertical channel, *Stat., Optim. Inf. Comput.*, Vol. 11, January 2023, p 55–69. DOI: 10.19139/soic-2310-5070-1725
- [5]. Chen H, Witharana S, Jina Y, Kim C, Ding Y. Predicting thermal conductivity of liquid suspensions of nanoparticles (nanofluids) based on rheology. *Particuology* 2009;7:151–7.
- [6]. Cheng, Ching-Yang. "Combined heat and mass transfer in natural convection flow from a vertical wavy surface in a power-law fluid saturated porous medium with thermal and mass stratification." *International Communications in Heat and Mass Transfer* 36, no. 4 (2009): 351-356. <https://doi.org/10.1016/j.icheatmasstransfer.2009.01.003>
- [7]. Cheng, Ching-Yang. "Double-diffusive natural convection along a vertical wavy truncated cone in non-Newtonian fluid saturated porous media with thermal and mass stratification." *International Communications in Heat and Mass Transfer* 35, no. 8 (2008): 985-990. <https://doi.org/10.1016/j.icheatmasstransfer.2008.04.007>
- [8]. Choi SUS. Enhancing thermal conductivity of a fluids with nanoparticles. *ASME Int* 1995;66:99–105.
- [9]. Choi, S. U. S., and Jeffrey A. Eastman. *Enhancing thermal conductivity of fluids with nanoparticles*. No. ANL/MSD/CP-84938; CONF-951135-29. Argonne National Lab.(ANL), Argonne, IL (United States), 1995.
- [10]. Das, S., and R. N. Jana. "Natural convective magneto-nanofluid flow and radiative heat transfer past a moving vertical plate." *Alexandria Engineering Journal* 54, no. 1 (2015): 55-64. <https://doi.org/10.1016/j.aej.2015.01.001>

- [11]. Das, S., R. N. Jana, and O. D. Makinde. "Transient natural convection in a vertical channel filled with nanofluids in the presence of thermal radiation." *Alexandria Engineering Journal* 55, no. 1 (2016): 253-262. <https://doi.org/10.1016/j.aej.2015.10.013>
- [12]. Devasena Y: Effect of non-linear thermal radiation, activation energy on hydromagnetic convective heat and mass transfer flow of nanofluid in vertical channel with brownian motion and thermophoresis in the presence of irregular heat sources, *World Journal of Engineering Research and Technology (JERT) wjert*, Vol. 9, Issue 2, XX-XX, (2023) ISSN 2454-695X, SJIF Impact Factor: 5.924, www.wjert.org
- [13]. Dhlamini M., Kameswaran P. K., Sibanda P., Motsa S., and Mondal H., *J. Comp. Design Eng.* 6, (2019)149.
- [14]. Duangthongsuk W, Wongwises S. Comparison of the effects of measured and computed thermophysical properties of nanofluids on heat transfer performance. *Exp Therm Fluid Sci* 2010;34:616–24.
- [15]. Fakour, M., Vahabzadeh, A., Ganji, D. D: Scrutiny of mixed convection flow of a nanofluid in a vertical channel, *Case Stud. Therm. Eng.* 4, pp.15-23(2014).
- [16]. Forsyth J.B., Hull S., The effect of hydrostatic pressure on the ambient temperature structure of CuO, *J. Phys.: Condens. Matter* 3 (1991) 5257–5261, doi:10.1088/0953-8984/3/28/001. Crystallographic point group: 2/m or C2h. Space group: C2/c. Lattice parameters: a = 4.6837(5), b = 3.4226(5), c = 5.1288(6),  $\alpha = 90^\circ$ ,  $\beta = 99.54(1)^\circ$ ,  $\gamma = 90^\circ$ .
- [17]. Gayathri .P: Impact of Variable Viscosity, Activation Energy on MHD Mixed convective Heat and Mass Transfer Flow of a Nanofluid in a Cylindrical Annulus, *YMER*, Vol.21 : Issue 4 ((April) – 2022), pp. 211-223, ISSN : 0044-0477, <http://ymerdigital.com>
- [18]. Glemser O. and Sauer H. (1963). "Copper, Silver, Gold". In G. Brauer (ed.). *Handbook of Preparative Inorganic Chemistry*, 2nd Ed. Vol. 1. NY, NY: Academic Press.
- [19]. Grosan, T., Pop, I: Fully developed mixed convection in a vertical channel filled by a nanofluid, *J. Heat Transfer* 134 (8), 082501(2012).
- [20]. Hatami, M., Hatami, J. and Ganji, D.D., "Computer, Simulation of MHD Blood Conveying Gold Nanoparticles as a Third Grade Non-Newtonian Nanofluid in a Hollow Porous Vessel," *Computer Methods and Programs in Biomedicine*, 113, pp. 632-641 (2014).
- [21]. Huang D, Liao F, Moles S, Redinger D, Subramanian V. 2003. Plastic-Compatible Low Resistance Printable Gold Nanoparticle Conductors for Flexible Electronics. *J. Electrochem. Soc.* 150(7):G412. <https://doi.org/10.1149/1.1582466>
- [22]. Kabeel AE, Maaty TAE, Samadony YE. The effect of using nano-particles on corrugated plate heat exchanger performance. *Appl Therm Eng* 2013;52:221–9.
- [23]. Kathyani,G and Venkata Subrahmanyam,P:Effect of dissipation on HD convective heat and mass transfer flow of thermally radiating nanofluid in vertical channel with activation energy and irregular heat sources. *MukthShabd Journal*, (2023), ISSN No.2347-3150,Scientific Journal;ISSN No:2347-3150,Vol.XII,Issue.III, pp.433-441
- [24]. Koffyberg F. P. and Benko F. A. (1982). "A photoelectrochemical determination of the position of the conduction and valence band edges of p-type CuO". *J. Appl. Phys.* 53 (2): 1173. Bibcode:1982JAP....53.1173K. doi:10.1063/1.330567.
- [25]. Kwak K, Kim C. Viscosity and thermal conductivity of copper oxide nanofluid dispersed in ethylene glycol. *Korea Aust Rheol J* 2005;17:35–40.
- [26]. Madduleti Nagasasikala, Bommana Lavanya : Effects of Dissipation and Radiation on Heat Transfer Flow of a Convective Rotating Cuo-Water Nano-fluid in a Vertical Channel, *Journal of Advanced Research in Fluid Mechanics and Thermal Sciences* 50, Issue 2 (2018) 108-117
- [27]. Maghrebi, M.J., Nazari, M., Armaghansi, T: Forced convection heat transfer of nanofluids in a porous channel, *Transp. Porous Media* 93, pp.401-413(2012).
- [28]. Mahajan A and Arora M. : Convection in rotating magnetic nanofluids. *Applied Mathematics and Computation*; V.219: (2013) pp..6284–6296.
- [29]. Mahanthesh, B., B. J. Gireesha, and Rama Subba Reddy Gorla. "Heat and mass transfer effects on the mixed convective flow of chemically reacting nanofluid past a moving/stationary vertical plate." *Alexandria Engineering Journal* 55, no. 1 (2016): 569-581. <https://doi.org/10.1016/j.aej.2016.01.022>
- [30]. Maïga, S.E.B., Nguyen, C.T., Galanis, N., Roy, G: Heat transfer behaviors of nanofluids in a uniformly heated tube, *Superlatt. Microstruct.* 35, pp.543-557(2004).
- [31]. Maïga, S.E.B., Palm, S.J., Nguyen, C.T., Roy, G., Galanis, N: Heat transfer enhancement by using nanofluids in forced convection flows, *Int. J. Heat and Fluid Flow* 26, pp.530-546(2005).
- [32]. Maleque K.A., , *ISRN Thermo.*, V.9, (2013).
- [33]. Mohamed Ouni a, Lotfi M. Ladhar b, Mohamed Omri c, Wasim Jamshed d, Mohamed R. Eid : Solar water-pump thermal analysis utilizing copper–gold/engine oil hybrid nanofluid flowing in parabolic trough solar collector: Thermal case study, *Case Studies in Thermal Engineering* 30 (2022) 101756, <https://doi.org/10.1016/j.csite.2022.101756>
- [34]. Nadeem S and Saleem S. : Unsteady mixed convection flow of nanofluid on a rotating cone with magnetic field. *Appl. Nanoscience*; V.4: (2014) pp.405-414.
- [35]. Nagasasikala M : Effect of activation energy on convective heat and mass transfer flow of dissipative nanofluid in vertical channel with Brownian motion and thermophoresis in the presence of irregular heat sources, *World Journal of Engineering Research and Technology (JERT) wjert*, (2023), Vol. 9, Issue 2, XX-XX, ISSN 2454-695X, SJIF Impact Factor: 5.924, www.wjert.org
- [36]. Netai Roy and Dulal Pal, : Influence of Activation Energy and Nonlinear Thermal Radiation with Ohmic Dissipation on Heat and Mass Transfer of a Casson Nanofluid Over Stretching Sheet, *Journal of Nanofluids*, Vol. 11, No. 6, (2022) pp. 819–832, doi:10.1166/jon.2022.1882, www.aspbs.com/jon
- [37]. Nield, D.A., Kuznetsov, A.V: Forced convection in a parallel -plate channel occupied by a nanofluid or a porous medium saturated by a nanofluid, *Int. J. Heat Mass Transfer*, 70, pp. 430-433(2014).
- [38]. Oztop H. F. and Abu-Nada E., "Numerical study of natural convection in partially heated rectangular enclosures filled with nanofluids," *International Journal of Heat and Fluid Flow*, vol. 29, no. 5, (2008)pp. 1326–1336.

- [39]. Peyghambarzadeh SM, Hashemabadi SH, Hoseini SM, Jamnani MS. Experimental study of heat transfer enhancement using water/ethylene glycol based nanofluids as a new coolant for car radiators. *Int J Heat Mass Transf* 2011;38:1283–90.
- [40]. Peyghambarzadeh SM, Hashemabadi SH, Naraki M, Vermahmoudi Y. Experimental study of overall heat transfer coefficient in the application of dilute nanofluids in the car radiator. *Appl Therm Eng* 2013;52:8–16.
- [41]. Rashidi, M. M., E. Momoniat, M. Ferdows, and A. Basiriparsa. "Lie group solution for free convective flow of a nanofluid past a chemically reacting horizontal plate in a porous media." *Mathematical Problems in Engineering* 2014 (2014). <https://doi.org/10.1155/2014/239082>
- [42]. Reddy, P. Chandra, M. C. Raju, and G. S. S. Raju. "Free Convective Heat and Mass Transfer Flow of Heat-Generating Nanofluid past a vertical moving porous plate in a Conducting field." *Special Topics & Reviews in Porous Media: An International Journal* 7, no. 2 (2016). <https://doi.org/10.1615/SpecialTopicsRevPorousMedia.2016016973>
- [43]. Richardson, H. Wayne (2002). "Copper Compounds". *Ullmann's Encyclopedia of Industrial Chemistry*. Weinheim: Wiley-VCH. doi:10.1002/14356007.a07\_567. ISBN 978-3527306732.
- [44]. Sacheti, N.C., Chandran, P., Singh, A.K., Bhadauria, B.S: Transient free convective flow of a nanofluid in a vertical channel, *Int. J. Energy Technol.* 4 pp. 1-7(2012).
- [45]. Sandeep, N., and M. Gnanaswara Reddy. "Heat transfer of nonlinear radiative magnetohydrodynamic Cu-water nanofluid flow over two different geometries." *Journal of Molecular Liquids* 225 (2017): 87-94. <https://doi.org/10.1016/j.molliq.2016.11.026>
- [46]. Satya Narayana K and Ramakrishna G N : Effect of variable viscosity, activation energy and irregular heat sources on convective heat and mass transfer flow of nanofluid in a channel with brownian motion and thermophoresis, *World Journal of Engineering Research and Technology (JERT) wjert*, (2023), Vol. 9, Issue 2, XX-XX, ISSN 2454-695X, SJIF Impact Factor: 5.924, www.wjert.org
- [47]. Shafiq Ahmad, Farhad Ali, Ilyas Khan, Sami Ul Haq : Biomedical applications of gold nanoparticles in thermofluids flow through a porous medium, *International Journal of Thermofluids* 20 (2023) 100425, <https://doi.org/10.1016/j.ijft.2023.100425>
- [48]. Sheikholeslami, M., Ganji, D.D: Magnetohydrodynamic flow in a permeable channel filled with nanofluid, *Sci. Iran. B* 21 (1), pp.203-212(2014).
- [49]. Sreedevi G and Prasada Rao D.R.V. "Effect of Dissipation and Radiation on Convective Heat Transfer Flow of a Rotating Cu-Water Nano-fluid in a Vertical Channel", *International Journal for Research and Development in Technology (IJRDT)*, Vol. 8(2) (2017) pp. 21-30.
- [50]. Sreedevi G, Prasada Rao D. R. V. & Raghavendra Rao R : Numerical Study of Convective Heat and Mass Transfer Flow in Channels, *Advances in Applied Mathematics, Springer Proceedings*, 2014, pp.115-125, DOI:10.1007/978-3-319-06923-4\_11
- [51]. Srinivas S, Vijayalakshmi A, Subramanyam Reddy A : Flow and heat transfer of gold-blood nanofluid in a Porous channel with moving/stationary walls, *Journal of Mechanics*, Vol. 33, No. 3, June 2017 395, DOI : 10.1017/jmech.2016.102
- [52]. Sudarsana Reddy P, Sreedevi P., Chamkha Ali J: MHD boundary layer flow, heat and mass transfer analysis over a rotating disk through porous medium saturated by Cu-water and Ag-water nanofluid with chemical reaction., *Powder Technology (Elsevier)*, Volume 307, 1 February 2017, Pages 46-55, <https://doi.org/10.1016/j.powtec.2016.11.017>
- [53]. Thompson DT. 2007. Using gold nanoparticles for catalysis. *Nano Today*. 2(4):40-43. [https://doi.org/10.1016/s1748-0132\(07\)70116-0](https://doi.org/10.1016/s1748-0132(07)70116-0)
- [54]. Umair Khan, Aurang Zaib, Anuar Ishak : Magnetic Field Effect on Sisko Fluid Flow Containing Gold Nanoparticles through a Porous Curved Surface in the Presence of Radiation and Partial Slip, *Mathematics* 2021, 9, 921. <https://doi.org/10.3390/math9090921>
- [55]. Zhou M, Xia G, Li J, Chai L, Zhou L. Analysis of factors influencing thermal conductivity and viscosity in different kinds of surfactant solutions. *Exp Therm Fluid Sci* 2012;36:22–9.